POLITECNICO DI TORINO

Master's Degree in Biomedical Engineering

Politecnico di Torino

Microneedle-Based Electrochemical Sensors for Real-Time Potassium and pH Monitoring

Supervisors
Sofia TEIXEIRA
Gianluca CIARDELLI

Candidate
Valeria CIOCE

Academic Year
2024/2025

INDEX

1. Introduction

1.1. Biosensors

Biosensors seamlessly merge advanced detection technology with the precision of specific biological elements, functioning as analytical tools that convert biological responses into

electrical signals.[1] Defined by the International Union of Pure and Applied Chemistry, biosensors are self-contained devices where a biological recognition element interacts closely with a transduction element, utilizing electrochemical, optical, or mechanical transducers.[2]

To ensure optimal performance, biosensors must exhibit high specificity, resilience to physical parameters like pH and temperature, and reusability.[3] Originally designed for point-of-care (POC) testing, biosensors aimed to extend clinical analysis beyond specialized laboratories, reaching diverse settings such as hospitals, non-hospital nursing environments, and homes.[4]

On the other hand, a chemical sensor is a device designed to convert chemical information—ranging from the concentration of a specific sample component to total composition analysis—into an analytically useful signal. Comprising a chemical recognition system (receptor) and a physicochemical transducer connected in series, chemical sensors typically consist of two integral components. Biosensors, falling under the broader category of chemical sensors, use a biochemical recognition system to interpret biochemical information, ensuring a high degree of selectivity for the specific analyte being measured.[5]

In living organisms/systems, such as olfaction, taste, and neurotransmission pathways, where cell receptors perform the actual recognition, the terms "receptor" or "bioreceptor" are often interchangeably used for the recognition system of a chemical biosensor. [2]

1.1.1. Types of biosensors

- *Enzyme biosensors* leverage various immobilization methods, including adsorption through van der Waals forces, ionic bonding, or covalent bonding. The enzymes typically employed in this process include oxidoreductases, polyphenol oxidases, peroxidases, and amino oxidases. These methods play a crucial role in creating effective and stable enzyme biosensor platforms.[6]
- *Tissue-based sensors* draw upon materials sourced from both plants and animals. These sensors are engineered to identify analytes that either impede or act as substrates in various biological processes within these tissues. On the other hand, organelle-based sensors utilize membranes, chloroplasts, mitochondria, and microsomes, providing a robust foundation with high stability. It's important to note, however, that these biosensors may come with a trade-off – while they offer heightened stability, they tend to exhibit longer detection times and a degree of reduced specificity. This calls for a careful balance when considering their application in different contexts.[7]

- *Immunosensors* have their foundation in the remarkable affinity that antibodies exhibit toward their corresponding antigens. In essence, these antibodies possess a high specificity, selectively binding to pathogens, toxins, or engaging with elements within the host's immune system. This unique interaction forms the basis for the establishment and functionality of immunosensors.[5]
- *DNA biosensors* capitalize on the fundamental property that a single-stranded nucleic acid molecule can discern and attach itself to its complementary strand within a given sample. This interaction is driven by the establishment of stable hydrogen bonds between the two nucleic acid strands. The specificity and selectivity inherent in the formation of these bonds underpin the functionality of DNA biosensors, making them valuable tools for molecular recognition in various applications.[5 8]
- *Magnetic biosensors*, harnessing the magnetoresistance effect, exhibit significant potential in terms of both sensitivity and size when detecting magnetic micro- and nanoparticles within microfluidic channels. This innovative approach offers the advantage of enhanced sensitivity while maintaining a compact form, showcasing promising prospects for diverse applications.[5]
- *Thermal biosensors*, also known as *calorimetric biosensors*, are crafted by incorporating biosensor materials, as previously mentioned, into a physical transducer. This integration of biological elements with a transducer allows for the conversion of biochemical reactions into measurable thermal signals. In essence, these biosensors leverage heat changes associated with specific biological interactions, offering a unique and sensitive method for detection and analysis.[9]
- *Piezoelectric biosensors* come in two main types: the quartz crystal microbalance and the surface acoustic wave device. These sensors operate by measuring alterations in the resonance frequency of a piezoelectric crystal, induced by changes in mass on the crystal structure. This ingenious approach allows for the sensitive detection of molecular interactions and provides a versatile platform for various aplications in biosensing.[8]
- *Optical biosensors* comprise a light source and multiple optical components designed to generate a light beam with specific characteristics. This light is then directed to a modulating agent through a modified sensing head, and the resulting interaction is detected by a photodetector. In essence, these biosensors utilize the principles of light modulation and detection to translate biochemical interactions into measurable signals, making them valuable tools for sensitive and real-time molecular analysis.[10]

- *Electrochemical biosensors* belong to the category of biosensors that measure electrical changes associated with biochemical reactions. These biosensors utilize electrodes and principles of electrochemistry to convert biochemical events into measurable electrical signals. The interaction between the biological or chemical target and the biochemical component on the electrode induces a change in electrical properties that can be detected and quantified.[6]

1.1.2. Characteristics of biosensors

- Selectivity: An essential factor in biosensor development, selectivity ensures the accurate identification of target analytes amidst complex mixtures and contaminants. Bioreceptors play a crucial role by selectively interacting with specific molecules in the sample, minimizing false positives and enhancing reliability.[11]
- Sensitivity: Reflecting the biosensor's ability to detect analytes, even at low concentrations, sensitivity is typically quantified in ng/mL or fg/mL. Enhanced sensitivity enables the detection of minute analyte quantities with minimal procedural steps, bolstering overall biosensor performance.[11]
- Linearity: This characteristic contributes to result accuracy by establishing a direct correlation between substrate concentration and detection response. Greater linearity indicates a more consistent and predictable response across a wide range of analyte concentrations.[12]
- Response Time: Representing the time required to achieve 95% of measurement results, response time signifies how quickly the biosensor can deliver actionable data. Swift response times are desirable, particularly in dynamic environments where real-time monitoring is crucial.[13]
- Reproducibility: Defined by precision and accuracy, reproducibility assesses the consistency of results across repeated measurements of the same sample. A highly reproducible biosensor generates consistent outputs with minimal variation, instilling confidence in its performance and reliability.[14]
- Stability: Vital for continuous monitoring applications, stability evaluates the biosensor's ability to withstand environmental changes and degradation over time. Factors such as the bioreceptor's affinity for the analyte and its susceptibility to degradation influence the biosensor's long-term stability and effectiveness in real-world applications.[13],[14]

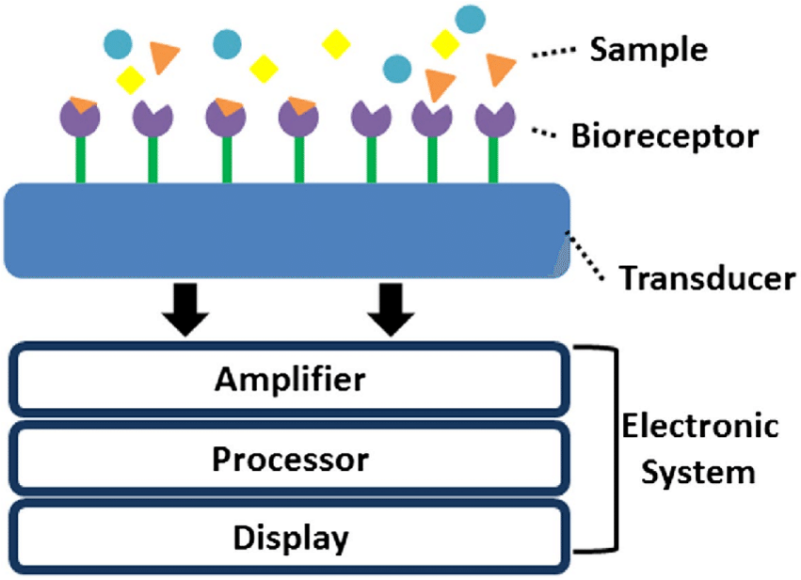

Figure 1 Schematic representation of a biosensor. [8]

1.1.3. Electrochemical biosensors

Electrochemical biosensors, composed of an electrochemical transducer, receptor, and detector, play a crucial role in medical science for analyzing bioanalytes. They offer convenient, accurate, POC detection of essential substances like glucose, lactic acid, cholesterol, and uric acid in bodily fluids. By detecting oxidation and reduction reaction potentials/gradients of associated enzymes/metabolites, Electrochemical biosensors convey electrochemical signals to electrodes for quantifying solute concentrations, thus enhancing drug delivery effectiveness in living organisms. With advancements in biomedical engineering and technology, wearable and implantable electrochemical sensor systems have emerged alongside POC sensing systems. [15]

1.1.4. Multiparameter electrochemical sensors

Multiparameter electrochemical sensors provide enhanced functionality, reduced complexity, and improved efficiency in data collection compared to single-parameter sensors.[15] In biomedical applications, they monitor physiological parameters like glucose, lactate, pH, and temperature in biological fluids, enabling continuous health monitoring and personalized medicine.[16] Integrating various sensing elements into a single platform, often with advanced materials and fabrication techniques, enhances performance across multiple parameters. These sensors offer versatile solutions for monitoring complex systems in environmental monitoring, healthcare, food safety, and industrial process control. Real-time monitoring of diverse

parameters offers dynamic insights into biological conditions, facilitating prompt interventions.[17] Multiplex biosensors find applications in diagnostic medicine, pharmaceutical research, and environmental analysis, contributing to economical resource usage. Understanding biosensor response provides valuable insights into sensitivity, selectivity, detection limit, and response time, ensuring reliable evaluations across diverse applications.[18]

Table 1 Examples of multiplexed electrochemical sensors

APPROACH	**RESULTS**
Platinum nanoparticles underwent modification with amino groups and paired with specific metal ions, forming hybrids. Linked to antibodies, these hybrids acted as distinctive tags for capturing substances.[19]	The sensor demonstrated notable precision in concurrently detecting cancer-related substances (CEA and AFP) within a defined concentration range: from 0.05 ng mL^{-1} to 200 ng mL^{-1} with a correlation coefficient of 0.997, and the detection limit of CEA was 0.002 ng mL^{-1}.
Gold and magnetic nanoparticles linked to specific peptides on a screen-printed carbon electrode allow simultaneous detection of two common food-borne pathogens. The presence of the bacteria's protease enzymes enables rapid detection within 1 minute. [20]	Detection of multiple bacteria simultaneously in a cost-effective manner, without the need for complex DNA extraction or amplification techniques. Linear responses were obtained from 10 to 10^7 colony-forming unit mL^{-1} for both bacteria.
A four-way junction hybridization is presented, one of the four adaptor strands is modified with a redox mediator facilitating detection, using an electrochemical biosensor.[21]	The LOD of this for SARS-CoV-2 which is 5.0 and 6.8 ng/μL respectively, is lower than the viral load in clinical samples so could be utilized to detect SARS-CoV-2 RNA fragments in the early stages of the disease when the viral load is still low.
An array-based flexible sensor platform in polymide was developed for the detection of multiple analytes. The flexible sensor array consists of a total of twelve working electrodes along with three reference and counter electrodes.[22]	Multi-biasing can be applied to detect analytes with different redox potentials and redundancy may mitigate signal reliability issues. the sensors are shown to have sensitivities of 26.31 μA $mM^{-1}\cdot cm^{-2}$ for glucose, 1.49 μA $mM^{-1}\cdot cm^{-2}$ for lactate, 54 $mV\cdot pH^{-1}$ for pH, and 0.002 $°C^{-1}$ for temperature.
Indium tin oxide (ITO) sheets were employed as working electrodes and graphene nanocomposites as supporting matrix for simultaneous determination of carcinoembryonic antigen (CEA) and α-fetoprotein (AFP). ITO was coated with graphene oxide for immobilization of anti-CEA.[23]	The proposed immunosensor avoided labeling either antigens or antibodies, simplified the operation and prevented the cross-talk between the different analytes. linear working ranges of 0.01–300 ng mL^{-1}. The limit of detections for CEA is 0.650 pg m^{-1} and for AFP is 0.885 pg mL^{-1}.
This design provides multiple immobilization areas, where the assay components are adsorbed, followed by their individual electrochemical cells, where the amperometric signal readout takes	The implementation and in-depth comparison of newly designed electrochemical multiplexed chip designs have been demonstrated. The sensors have very similar LODs of

place, within a single microfluidic channel. The immobilization area and electrochemical cell are strictly separate to not avoid sensitivity.[24]	22.5 ng mL^{-1} and 28.6 ng mL^{-1} for single analyte/sample and, multiplex respectively.

1.2. Microneedles biosensors

Microneedles are micron-scale needles that generally range from 25 to 2500 μm in length, 20 to 250 μm in width, and 1 to 25 μm in tip diameter, which can be arranged as individual needles[25], a row of needles, or needle array patches depending on the applications.

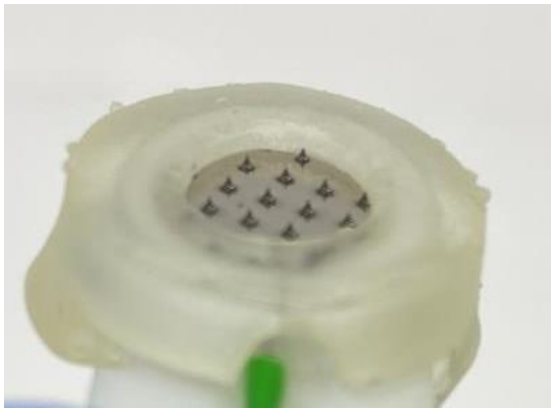

Figure 2 Microneedle-based platinum sensor.

Microneedles represent a significant advancement in POC diagnostics, offering a less invasive alternative to traditional blood sampling. These microscale needles play a vital role in reshaping diagnostic methodologies, addressing the need for less uncomfortable and complex sampling methods.[26] Researchers are actively developing swift and cost-effective POC diagnostic devices, exploring easily accessible body fluids like interstitial fluid (ISF), urine, and saliva as alternatives to blood. ISF, similar in composition to plasma, allows for continuous monitoring of various biomarkers, revolutionizing blood-based clinical care.[27] Conventional ISF sampling methods grapple with limitations in POC diagnosis, including insufficient volume (1-10 μL) and filtration issues.[25] Microneedle technologies hold promise in reshaping diagnostic procedures, serving as a conduit between innovation and practical healthcare applications. These needles puncture micro-holes in the skin, bypassing blood capillaries and promoting rapid healing within minutes. Due to varying ISF concentrations across skin layers, the dermis is ideal for microneedle sensing. Diagnostic devices predominantly utilize microneedle arrays with biochemical sensors, ensuring a comfortable and minimally invasive sampling experience.[27]

Challenges persist in biosensor adoption, particularly regarding stability and miniaturization. Continuous monitoring of electrolyte levels is essential for timely disease diagnosis and

monitoring. Therefore, a mechanically robust and multiplexed microneedle-based sensor capable of continuously monitoring multiple electrolytes is essential for understanding dynamic variations. Materials used in microneedles must meet specific criteria, including biocompatibility, appropriate dimensions, and mechanical strength. Electrical and electrochemical properties, along with biorecognition components, are essential for accurately converting chemical signals into measurable ones in biosensors. Additionally, attributes like biodegradability and antifouling properties contribute to enhancing biosensor performance and reliability for various applications. These microneedles, available in solid, hollow, coated, and dissolvable configurations, curtail contact with nerve terminals, ensuring a comfortable sampling experience.[28]

2.1.1. *Types of microneedles*

- *Solid microneedles*: The microneedle structure is designed to penetrate the stratum corneum for improved bioavailability and skin transport forming micron-scaled pores on the skin surface. Solid microneedles, ideal for vaccine delivery, offer prolonged effectiveness and a stronger antibody response compared to intramuscular delivery. They are easy to manufacture, possess superior mechanical properties, and sharper tips than hollow microneedles. Solid microneedles can be fabricated from different materials, providing versatility for different applications.[29]
- *Hollow microneedles*: The hollow microneedle features a design with an empty core for storing and injecting drug fluid. This design allows for drug delivery into the viable epidermis or dermis, making it suitable for high molecular weight compounds. Hollow microneedles also enable controlled drug release over time, particularly effective for liquid vaccine formulations. Serving as an active drug delivery system, they act as a conduit for drug diffusion into the dermis from a non-pressurized drug reservoir. The tunable release kinetics of hollow microneedles can be adjusted by leveraging both material formulation and fabrication parameters.[30]
- *Dissolving microneedles*: characteristics of dissolvable MNs include their ability to facilitate the rapid release of macromolecules, providing a one-step drug application that enhances ease of drug administration. The dissolvable MN tip can be loaded efficiently using a two-step casting method. Upon insertion into the skin, the drug is released and diffuses easily as the needle tip dissolves. Water-soluble materials are most suitable for manufacturing dissolvable MNs, with the micro-mold method being the preferred fabrication technique. However, it's worth noting that complete insertion

of this type of MN can be challenging, and there may be a delay in the dissolution process.[31]

Table 2 Examples of multiplexed microneedle-based electrochemical sensors

ABOUT	RESULTS
MNs made of a polymer matrix of crosslinked methacrylated hyaluronic acid (MeHA) was produced, blended with hyaluronic acid (HA) to enhance the extraction of ISF through the application of a mechanical strength. Four working electrodes are modified with specific enzyme or sensing reagent to achieve selective detection of respective substrates.[32]	An artificial skin model was used to show that the sensitivity and detection range of the sensors are sufficient for diagnosis purposes. Then a mouse model was used to demonstrate the feasibility of early diagnosis. The sensors are able to give for phosphate a sensitivity of 50–550 μM, for uric acid of 4.19 nA/μM, 12.58 nA/μM for creatinine and 44.6 mV/decade for urea.[32]
Flexible microneedle electrode array-based biosensor (MEAB) and a multi-channel portable electrochemical analyzer (MPEA) were fabricated. Needles modified through bio-functionalization of the microneedle electrode array (MEA) with glucose oxidase (GOx), uricase (UOx) and cholesterol oxidase (ChOx) for simultaneous detection of glucose, uric acid and cholesterol levels in serum.[33]	The analytes in serum samples were measured by MPEA and PED in parallel. Analysis was performed to check the detection consistency of MPEA demonstrated excellent sensing performance with a wide linear range (glucose, 2–12 mM; uric acid, 0.1–1.2 mM; cholesterol, 1–12 mM), low detection limit (glucose, 260 μM; uric acid, 4 μM; cholesterol, 440 μM), and rapid response time (∼4 s).
A multiplexed sensors were fabricated via layer-by-layer (LbL) assembly on a PDMS microneedle platform coated with a conductive PDMS/carbon nanotube (CNT)/cellulose nanocrystal (CNC) composite.[34]	Each sensor rapidly (~2 min) and selectively responded to their target analytes, with excellent precision between scans. The limits of detection (LOD) for the epinephrine, dopamine, and lactate sensors were 0.0007 ± 0.0002 μM, 2.11 ± 0.05 nM, and 0.07 ± 0.07 mM, respectively. The pH sensor accurately responded to a pH range of 4.25–10.
This is a minimally invasive microneedle-based potentiometric sensing system for multiplexed and continuous monitoring of Na^+ and K^+ in the skin ISFs. The potentiometric sensing system consists of a miniaturized stainless-steel hollow microneedle to prevent sensor delamination and a set of modified microneedle electrodes for multiplex monitoring.[28]	Here the electrochemical performance of Na^+ and K^+ sensors in artificial ISFs. For sodium the sensitivity is 56.08 mV/decade; R^2: 0.991. For potassium the sensitivity is 50.03 mV/decade; R^2: 0.999. The Na+ and K+ sensor data show that the potentiometric sensor exhibits rapid responses and negligible carry-over effects for different ion concentration levels.
High-density silicon microneedles are used to prepare a three-electrode patch for the electrochemical monitoring of glucose. The surface of the Si MNA was initially coated with an thin layer of gold and subsequently modified to conjugate dendrimers containing a redox mediator and the catalytic bioreceptor glucose oxidase (GOx).[35]	The MNA glucose patch shows very good selectivity when tested in artificial ISF, with a sensitivity of 0.1622 μA mm^{-1} cm^{-2} and a detection limit of 0.66 mm. In vivo application of the microneedle array in mice shows that the ISF glucose concentrations obtained with the MNA sensor gave very good

	correlation with the blood glucose levels determined with a commercial glucometer.
Multimodal hollow microneedle sensor array relies on unmodified and organophosphorus hydrolase (OPH) enzyme-modified carbon paste (CP) microneedle electrodes for square wave voltammetric (SWV) detection of the fentanyl and nerve agent targets, respectively. [36]	Two well-separated anodic morphine peaks are observed at +0.2V and +0.7V, corresponding to the pseudo-morphine generation and oxidative dealkylation of piperidine tertiary amine, respectively. As expected for amine-containing redox reactions, both morphine and fentanyl contribute to the oxidative current at +0.7V when using a mixture of these drugs; however, these drugs can be separated based on the morphine peak at +0.2V.

1.3. Interstitial fluid

Interstitial fluid, placed around body cells, serves as a reservoir of valuable biochemical information. Despite the promising insights ISF can offer, accessing this fluid is hindered by the skin's physical barrier. [37] Fortunately, MNs emerge as a solution, effortlessly surmounting this obstacle to access ISF in a painless and efficient manner. Distinguished by their microscale dimensions, microneedles present a minimally invasive method. The approach involves painless skin insertion, ensuring easy on-body portability and the potential for continuous biomarker monitoring.[27]

Here key analytes traditionally evaluated, their detection relevance and main diseases with which they are associated. [37]

Table 3 Analytes traditionally evaluated in ISF

Analyte	**Priority**	**Related diseases**
Sodium	Medium-high	Fluid loss, cystic fibrosis[38]
Potassium	Medium	Arrhythmia, renal failure, sepsis, reduced gut motility, cystic fibrosis, spreading depression[38]
Chloride	High	Sodium and acid-base disturbances, cystic fibrosis, spreading depression[39]
pH	High	Metabolic and respiratory acidosis, sepsis, spreading depression[38]
Calcium	High	Coagulopathy, osteopenia, neuromuscular excitability, cardiovascular complications[39]

1.3.1. Potassium

Potassium, a vital electrolyte crucial for cellular and electrical functions, is the primary positive ion within cells, constituting over 90% of the total body potassium stores. Teaming up with sodium, potassium regulates water and acid-base balance, playing a fundamental role in transmitting electrical impulses in the heart.[38] The active transport of potassium into and out of cells is indispensable for cardiovascular and nerve functions. As potassium enters cells, it triggers a sodium-potassium exchange across the cell membrane, creating electrical potential for nerve impulse conduction. Upon exiting the cell, potassium restores repolarization, enabling the progression of nerve impulses. This electrical potential gradient is also instrumental in influencing muscle contractions and regulating the heartbeat. Normal serum potassium levels fall between 3.6 and 5.0 mmol/L. Even a slight 1% decline in total body potassium (35 mmol) can result in a significant imbalance between intracellular and extracellular potassium, affecting the electrophysiologic properties of the cell membrane. Such an imbalance can have adverse effects on impulse generation and conduction throughout the heart. Studies on potassium deficiency, or hypokalemia, underscore its significance in cardiovascular disease (CVD). Increasing evidence suggests that elevated potassium intake may play a pivotal role in reducing blood pressure and lowering the risk of stroke, congestive heart failure (CHF), and cardiac arrhythmias.[40]

Most of the consumed potassium is primarily excreted through urine, making up around 80% to 90% of the total elimination. The remaining 10% to 20% is expelled through feces and sweat. Following filtration in the kidney glomerulus, the majority of the filtered potassium is reabsorbed along the kidney tubules. Increased extracellular potassium concentrations stimulate the release of aldosterone, a hormone that boosts the distal tubular secretion of potassium into the urine. Moreover, blood potassium levels undergo independent circadian rhythm control, resulting in higher excretion of dietary potassium during daylight hours compared to nighttime.[41]

1.3.2. Sodium

Sodium, an essential electrolyte, carries an electric charge in bodily fluids like blood. It plays a crucial role in maintaining fluid balance around cells, supporting normal nerve and muscle function. Sodium is acquired through food and drink and exits primarily through sweat and urine. Healthy kidneys regulate sodium levels by adjusting excretion in urine, preventing imbalances like hyponatremia (low sodium) or hypernatremia (high sodium). A significant function of sodium is its involvement in water balance, impacting blood pressure control.

Alongside chloride and potassium, sodium forms specific channels in cell membranes, overseeing vital tasks such as controlling water movement, facilitating nutrient transport into cells, and enabling muscle and heart contractions. It also supports nerve impulses for communication between the brain and the body. In extracellular fluid (ECF), sodium is the major cation, equivalent to 1 mmol (23 mg). In adult males, total body sodium averages 92 g, distributed with 46 g in ECF (concentration: 135–145 mmol/L), around 11 g in intracellular fluid (concentration: ~10 mmol/L), and approximately 35 g in the skeleton.[42] The sodium–potassium pump, fueled by ATP, maintains the concentration gradient between ECF and intracellular fluid. Specific channels or transport mechanisms in polarized cells facilitate sodium entry, with the pump expelling sodium into adjacent capillaries. Sodium transport in these cells is closely associated with other substrates, including phosphates, amino acids, glucose, and galactose. [43]

1.3.3. pH

The pH of body fluids is regulated by protons (H^+) generated from organic acids within living cells. Lactic acid ($lactate^-/H^+$) is a significant proton source, crucial for maintaining physiological pH. Metabolic tissues, like skeletal muscle and adipose tissue, undergo glycolytic anaerobic metabolism, converting glucose and glycogen into lactic acid. With a pKa of 3.80, lactic acid readily dissociates into lactate ($lactate^-$) and protons, causing a decrease in intracellular pH. Pyruvic acid ($pyruvate^-/H^+$), an intermediate metabolite in glycolysis, also serves as a proton source, generating fewer protons than lactic acid. [44] Additionally, ketone bodies contribute to the pool of proton sources. Protons from organic acids undergo partial buffering within cells. Unbuffered protons traverse the plasma membrane into extracellular fluid, where they are buffered in circulation or expelled through urine and exhaled gas. Crucial transporters, including monocarboxylate transporters and Na^+/H^+ exchangers, manage proton uptake and release across plasma membranes in metabolic tissue cells (e.g., skeletal muscle, liver), actively contributing to preserving physiological pH.[45] Dysfunctional transporters can lead to cellular impairment, diseases, and decreased physical performance due to abnormal pH. The pH in the interstitial space of metabolic tissues is easily altered due to limited buffering capacity, potentially triggering insulin resistance. This phenomenon is not observed in blood, which contains pH buffers like hemoglobin (Hb) and albumin. Regular exercise and dietary interventions regulate transporter expression and activity, aiding in maintaining bodily fluid pH. This underscores the positive impact of a healthy lifestyle, including exercise and dietary habits, on disease prognosis. [46]

1.4. Electrochemical sensing technology

To enable real-time analysis of body fluids during extraction, integrating MNs with electrochemical sensing technology is crucial. MNs can either incorporate electrodes or be designed as electrodes themselves using conductive materials. Detecting agents like enzymes and chemical catalysts can be immobilized on MNs through coating, blending, or covalent bonding. When these engineered MNs penetrate the skin, they initiate detection-relevant redox reactions, interacting with biomarkers in the target fluid. This chemical reaction generates an electrical signal, interpretable by a detection instrument, seamlessly integrating microneedle-based extraction and electrochemical sensing for on-site analysis. The electrode within an electrochemical sensor plays a pivotal role in facilitating and detecting redox reactions in a standard three-electrode system. This system comprises a working electrode, where the electrochemical reaction occurs with modifications to catalyze specific reactions; a counter electrode, ensuring smooth electron flow to complete the circuit; and a reference electrode, maintaining a constant potential for accurate measurements.[3]

To evaluate system reliability, immersion in solutions of known analytes concentrations aids in calibration and assessing precision and accuracy. As the system evolves, there may be a transition to in vivo applications, necessitating further adaptation for efficacy and safety within a biological environment. This includes considerations of miniaturization and accounting for biological influences on measurements. For in vivo monitoring, it could be considered a shift from the traditional three-electrode system to microneedle-based sensors. Microneedles serve multiple functions, acting as working electrodes modified to catalyze reactions and detect electrochemical changes related to analytes in interstitial fluid. This shift enhances accessibility, user comfort, and enables continuous monitoring in various diagnostic and healthcare scenarios.[15] Electrochemical techniques are commonly categorized into voltammetric and amperometric methods, among others.[45]

1.4.1. Ion-selective sensors

Ion-selective electrodes determine analyte concentrations by measuring the potential difference between working and reference electrodes at various analyte concentrations. These sensors detect the accumulation of a charge potential at the working electrode compared to the reference electrode in an electrochemical cell where no current flows between them. [22]

The relationship between concentration and potential is described by a variation of the Nernst equation:

$$E = E_0 \pm \frac{RY}{nF} lna_1$$

where, $E0$ represents the standard potential when $a_1 = 1$, R is the universal gas constant, T is the absolute temperature in Kelvin, $n$is the total number of charges on the ion, F is the Faraday constant, and $a1$ denotes the analyte activity. [47]

1.5. Electroanalytical techniques

Electroanalytical techniques are highly favored for exploring the redox reactions of organic and inorganic species. They excel in providing detailed insights into electrochemical processes with minimal time and effort spent on data collection and analysis.[15]

Furthermore, these techniques offer rapid responses after electrode stimulation, making them suitable for investigating mechanisms involving swift reactions and detecting short-lived transient intermediates.

The setup for these electrochemical techniques typically involves a working electrode submerged in a solution containing an excess of supporting electrolyte to prevent the migration of charged reactants and products. This setup facilitates the study of redox reactions to gain insights into the concentration of the solution. Additionally, it can be utilized to electrodeposit materials onto the electrode surface, enhancing selectivity for specific analytes.[48]

1.5.1. Cyclic voltammetry

CV is a dynamic electrochemical technique used to analyze oxidizable and reducible substances in solution. In CV, the potential of the working electrode cycles between two values while measuring the resulting current. This potential cycling is controlled relative to a reference electrode, such as a saturated calomel electrode (SCE) or a silver/silver chloride electrode (Ag/AgCl), which serves as the excitation signal.[49]

The excitation signal typically follows a linear potential scan with a triangular waveform, oscillating the electrode potential between specified switching potentials. The scan rate, measured in millivolts per second (mV/s), determines the slope of the scan.[48]

During the potential scan, the current at the working electrode is recorded, creating a cyclic voltammogram. This current serves as the response signal to the excitation signal and is plotted

against the potential on a graph. Modern instrumentation allows for easy adjustment of switching potentials and scan rates to suit experimental needs.[3]

CV applies a triangular waveform to the working electrode. Initially, the electrode potential undergoes a linear variation with time, however, the direction of the potential scan is reversed, resulting in the waveform combining two opposing linear sweeps. The resulting shape of the CV curve typically resembles a series of peaks and valleys, representing the oxidation and reduction processes of the electroactive species at the electrode surface.

CV is used to determine the nature of the redox reactions that take place in a solution. This

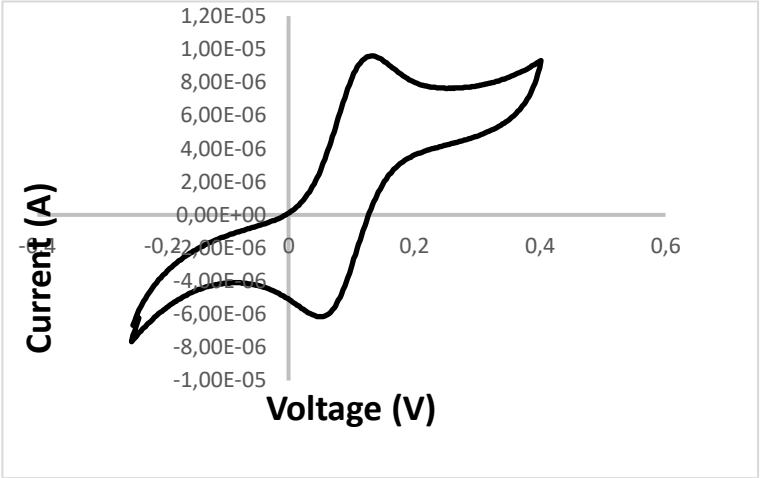

strategy, although not as sensitive as the pulse techniques, has a multitude of uses beyond the trace determination of an analyte such as the study of oxidation/reduction mechanisms, to detect biologically active molecules, the determination of formal potentials, electron transfer and electron transfer kinetics.[50]

Moreover, CV is widely used to modified electrodes with electro-active conducting polymers like polypyrrole, polyaniline, polythiophene, polyaniline (PANI), and other materials such as Iridium Oxide (IrOx).[49]

1.5.2. Square Wave Voltammetry

Among various voltammetric methods, square-wave voltammetry (SWV) stands out due to its exceptional sensitivity and rapidity. Its high-speed capabilities, combined with computerized control and signal averaging, enable repetitive experiments and enhance the signal-to-noise ratio.[50]

Figure 3. Shape of a CV voltammogram.

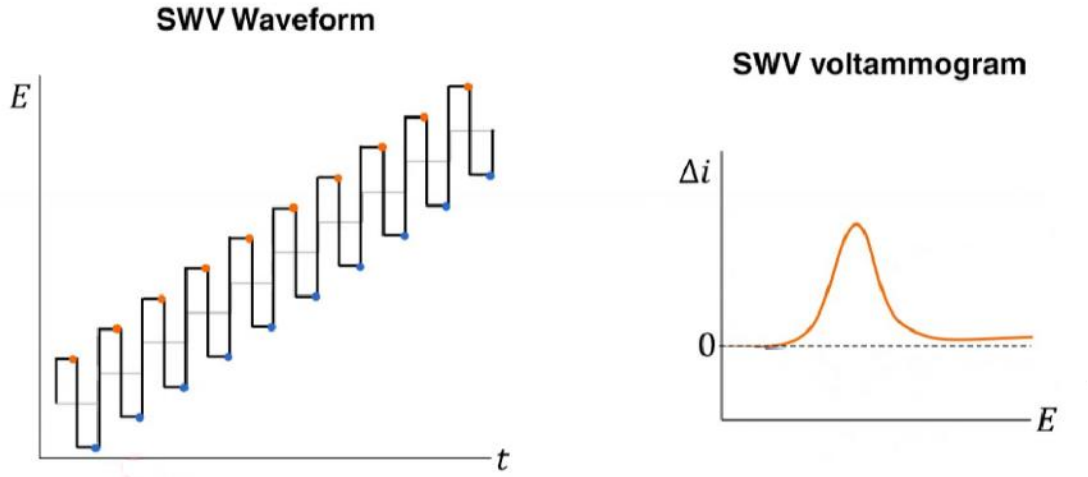

Figure 4. Wave form applied by a Square Wave Voltammetry and the resulting shape of the voltammogram. [51]

The waveform of SWV is a symmetrical square wave on a staircase SWV and can be applied for the analysis of reversible and irreversible reactions, reaction with slow electron transfer. When compared to linear sweep and cyclic voltammetry, SWV is a pulsed method, so offers a broader dynamic range and lower detection limits, thanks to its effective discrimination of capacitance current. The setup involves immersing the system in a solution with incrementally increasing concentrations of analytes. As the analyte's concentration rises, there's a corresponding increase in the current values detected. SWV's exceptional sensitivity and rapidity make it particularly well-suited for this purpose, allowing for precise and efficient determination of concentration levels. [51]

1.5.3. Open Circuit Potential

Open Circuit Potential (OCP) measurement entails determining the potential difference between a working electrode and a reference electrode without applying any potential or current. This technique offers several advantages over voltammetry and amperometry. It operates in a two-electrode mode, simplifying the setup with just working and reference electrodes. OCP allows for spontaneous measurement of electrode potential, enabling miniaturization of the reference electrode and facilitating simultaneous acquisition of multiple electrode potentials. Additionally, since OCP measures all redox reactions without applying voltage, it is less susceptible to interference from contaminants. Consequently, OCP can streamline electrochemical systems for use in both laboratory settings and clinical diagnostics.[52]

OCP measurement is passive, bypassing the circuitry of the potentiostat's counter electrode and only measuring the potential difference between the reference (E_{REF}) and working (E_{WKG}) electrodes.[22]

$$E_{OCP} = E_{WKG} - E_{REF}$$

This measurement reflects the system's electrochemical behavior, indicating stability if the OCP remains constant (typically within ±5 mV) over extended periods. A stable OCP suggests that the system is thermodynamically stable enough for perturbation-based experiments, offering greater analytical certainty compared to fluctuating readings.[52]

1.5.4. Chronoamperometry

Chronoamperometry, a dynamic electroanalytical technique, involves applying a constant potential to the working electrode, initiating a time-dependent process. This method monitors the evolving current at the electrode as analytes diffuse from the bulk solution towards the sensor surface. By examining the current-time relationship, chronoamperometry provides insights into the diffusion-controlled process, which varies with analyte concentration. Remarkably, it's a sensitive method that doesn't require labeling of the analyte or bioreceptor, finding utility in various studies, either independently or in conjunction with other electrochemical techniques.[53]

Chronoamperometry focuses on analyte transfer between the electrode and the electrochemical solution. This versatile technique finds applications in electrodeposition, particularly with the electroactive polymer Poly(3,4-ethylenedioxythiophene) (PEDOT).[15]

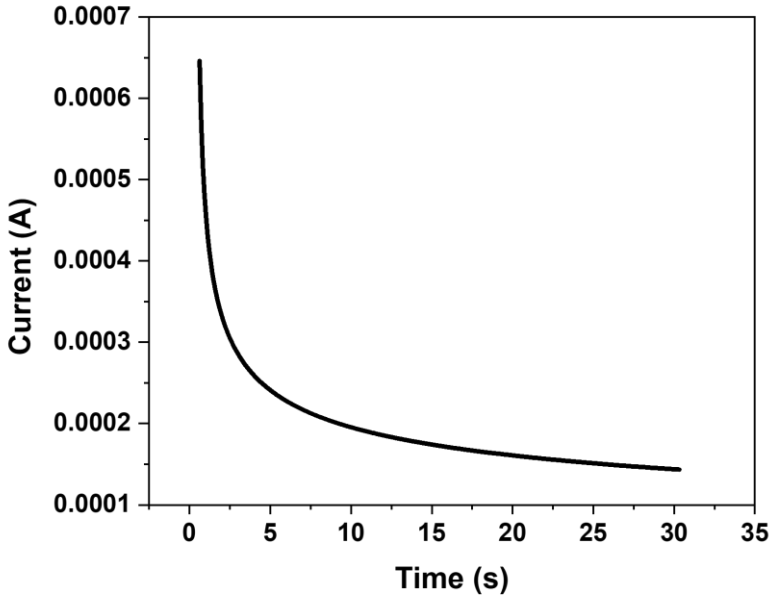

Figure 5. Chronoamperometry performed for 30 seconds.

1.6. Surface characterization

Considering the functional mechanism of biosensors, surface modification of the electrode is vital to biosensor performance.

1.6.1. PEDOT

PEDOT, renowned for its electrochemical properties, stability, and biocompatibility, is a conductive polymer widely employed in electrochemical applications. Electrodeposited onto surfaces, it alters their properties, making them suitable for diverse sensing and biosensing applications. Coating microelectrodes with conductive polymers (CPs) is a recognized method for enhancing the electrical characteristics of metallic surfaces. This enhancement is generally achieved through electrochemical deposition. CPs expand the electroactive surface area, resulting in a notable reduction in electrochemical impedance. This improvement is advantageous for boosting the signal-to-noise ratio (SNR) in in vivo neural recordings. Additionally, CPs offer excellent electrochemical attributes, increased stability, and proven biocompatibility.[54]

1.6.2. Ion Selective Membrane

Ion selective membranes (ISMs) are specialized membranes that allow specific ions to pass through based on their charge and size while blocking others. They are frequently utilized in

electrochemical sensors to enhance selectivity and specificity for targeted ions like potassium or sodium.[27]

Inspired by the natural membranes, the key players responsible for controlling ion transfer through ISMs are acceptor/ionophore components and nanopores/nanochannel. Clinical uses of these membranes encompass the creation of electrodes for precise and efficient detection and measurement of H^+, gases like CO_2 and O_2, metabolites such as urea, glucose, uric acid, lactate, and electrolytes like Na^+, Ca^{2+}, and K^+ in biological samples. This facilitates swift diagnoses of conditions like nutritional deficiencies, cardiac issues, respiratory ailments, and renal failure.[55]

1.6.3. Iridium Oxide

Iridium oxide (IrOx) is an inorganic compound composed of iridium and oxygen. This material is recognised for its exceptional hardness and corrosion resistance, making it a crucial element in various industrial and technological applications. Iridium oxide finds several significant applications. Due to its good electrical conductivity and corrosion resistance, it is often employed to modify electrodes in electrochemical sensor applications. IrOx potential shows strong pH dependence, exhibit excellent mechanical stability and biocompatibility, both of which allow for long-term implantation with minimal damage to living tissue.[34]

Electrodeposition of IrOx offers a controlled and versatile method to tailor the properties of electrode surfaces, making it suitable for various analytical, sensing, and biomedical applications. It allows researchers to optimize the material properties according to specific application requirements, ensuring reliable and efficient performance in the intended application.[56]

1.6.4. Polyaniline

Polyaniline (PANI), a versatile conducting polymer, offers significant potential for binding biomolecules, enhancing their bio-catalytic properties, facilitating rapid electron transfer, and enabling direct communication to generate various analytical signals and innovative analytical applications. This polymer has garnered substantial interest due to its unique and adjustable chemical and electrical properties, environmental and thermal stability, as well as its intriguing electrochemical, electronic, optical, and electro-optical characteristics. Its structural flexibility allows for a broad spectrum of tunable properties, leading to diverse applications in areas like

anti-corrosive coatings, energy storage systems, gas sensing, and electrochromic and electrocatalytic devices.[34]

Studies have highlighted PANI's superior environmental stability, making it the only conducting polymer stable in air. Its electroactivity enables PANI to serve as an effective mediator for electron transfer in redox or enzymatic reactions and provides a suitable matrix for the immobilization of biomolecules. These properties, along with its favorable storage stability and straightforward synthesis methods, have contributed to PANI's rising popularity in biosensor applications. Additionally, PANI offers benefits such as signal amplification and reduced electrode fouling, further emphasizing its potential in the field of biosensors. [57]

1.7. Aims and objectives

The project aimed to develop microneedle-based sensors capable of detecting various analytes, with a particular focus on pH and potassium. The pH sensors had been surface-modified using PANI or IrOx, while the potassium sensors had been enhanced with PEDOT and ion-selective membranes to improve their functionalities. These analytes are pivotal in biological systems, making their accurate monitoring essential for understanding physiological processes and diagnosing various health conditions. Deviations from optimal pH levels can indicate underlying health issues, underscoring the importance of precise pH monitoring for early detection and intervention. Similarly, abnormal potassium levels can lead to serious health complications, making its accurate measurement vital for managing conditions like hypertension, kidney disease, and cardiac arrhythmias.

The project aimed to make the measurement of specific analytes more portable and versatile by transitioning from an external setup using commercial electrodes to an on-patch setup, defined as internal, using exclusively microneedle-based sensors.

Microneedle technology represents a significant advancement in sensor development, enabling in vivo monitoring in a non-invasive manner.

Envisioned as a multi-parametric sensor capable of simultaneous detection of multiple analytes, time constraints led to a prioritization of specific analytes. Consequently, the developed software required further refinement to fully meet the project's objectives.

This research aims to address the growing demand for sensitive and selective sensors for real-time monitoring in various applications, including healthcare and environmental monitoring. By leveraging the unique properties of microneedle-based sensors, such as enhanced surface area and improved sensitivity, this project seeks to contribute to advancements in electrochemical sensing technologies.

As technology continues to evolve, the potential for multi-parametric sensors to revolutionize data collection and analysis remains a promising avenue for exploration.

2. Materials and Methods

2.1. Materials and reagents

The molds were prepared with Sylgard 184, part A and part B. The wafers were prepared with epoxy material, specifically EpoTek 353ND 1LB Kit, consisting of two components: Part A and Part B. NOA68 for Norland Optical Adhesive 68 LOT 369 produced by Norland Productions Inc was used for passivation. Phosphate Buffered Saline (PBS), ferrocene carboxylic acid (FCA), potassium chloride (KCl), hydrogen chloride (HCl), sodium hydroxide (NaOH), sodium chloride (NaCl) was purchased from Sigma Aldrich (Arklow, Ireland) Artificial Interstitial Fluid (ISF) was prepared with calcium chloride, HEPES, potassium chloride, magnesium sulfate, sodium chloride, sodium phosphate, sucrose purchased from Sigma Aldrich (Arklow, Ireland). Electrochemical measurements of the surface were performed using an aqueous reference electrode (Ag/AgCl) and platinum (Pt) auxiliary electrode.

2.1.1. Iridium Oxide

Iridium Oxide (IrOx) is synthesized following Yamanaka method[58] by first preparing a solution with 0.14 g of Iridium Chloride Hydrate at 99.95% purity, stirred for 30 minutes. Next, 1 ml of Hydrogen Peroxide solution is added, and the solution is stirred for an additional 10 minutes. Following this, 0.5 g of Oxalic Acid is added and stirred for another 10 minutes. Finally, Potassium Carbonate is gradually added to adjust the pH to 10.5.

2.1.2. PEDOT

Poly(3,4-ethylenedioxythiophene), commonly referred to as PEDOT, is synthesized by initially preparing a 0.1M potassium chloride solution (KCl). Subsequently, 1ml of PEDOT is thoroughly mixed into the 0.1M KCl solution to produce a 0.01M PEDOT solution.

2.1.3. Ion Selective Membrane

An ions selective membrane was prepared for potassium, mixing 0.014g of potassium Ionophore, 0.003g of potassium tetrakis chloroborate, 0.328g of Poly Vinyl Chloride and 0.63ml of 2 – nitrophenyloctyl ether. The membrane cocktail was dissolved in TetraHyddro furan. The cocktail was vortexed to ensure homogeneous solution and stored at 4 °C. The

solution was then applied to the surface of the working electrode, which was positioned on a wet bed. This setup was left overnight in a fume hood.

2.1.4. Polyaniline

A 0.1 M aniline solution was prepared in 2.5 M H_2SO_4.

2.1.5. Stock Solutions K^+

To conduct calibration studies, dilutions of various uniform concentrations were necessary. This involved preparing 200 mM calcium chloride solution. and serial dilutions were prepared in the following sequence: 1mM, 2.5mM, 5mM, 10mM, 15mM, 25mM, 50mM, 75mM, 100mM, 150mM, and 200mM.

2.2. Fabrication of Moulds

To make each mold, Sylgard parts A and B are used in a 10:1 ratio, 40 and 4 grams respectively. The two parts are mixed until the mixture is homogeneous. To degas the mixture, it is left to rest for 1 hour at room temperature. Then, it is poured into a mold, which is left overnight on a labeling table until it solidifies. After complete solidification, the mold is carefully removed.

2.3. Fabrication of wafers

To make the wafers, Epoxy parts A and B are used in a 10:1 ratio, 7 and 0.7 grams respectively. The two parts are mixed in a petri dish until the compound has a uniform yellow color. The solution is poured onto the back part of the mold, ensuring it covers all the needles.

2.3.1. Degassing

The front part of the mold with the solution is placed inside the Vacuum Chamber, ensuring that the plate it rests on is perfectly horizontal to degas the solution properly. Once the chamber door is closed, the pressure gauge and pump are turned on. Turn off the machine once the pressure reaches a value below the 150 mTorr.

Next, the back part of the mold is overlaid onto the front part, taking care not to create too much pressure to avoid solution spillage. It is then important to remove all bubbles, especially from areas where the arrays are present. The overlaid molds are placed under the hood, with the needles facing downwards, and the vacuum is turned on, with a weight on top for 15 minutes.

2.3.2. Curing

The molds are placed in the oven at 80°C for 1 hour. After reaching room temperature, the molds are carefully opened in a direction that allows accessing the array cavity first. To verify the conductivity of the arrays, slight pressure is applied to partially detach them from the wafer. Cleaning of the wafers is performed using a nitrogen gun and isopropanol. The wafer is then stored in a holder with the needles facing downwards.

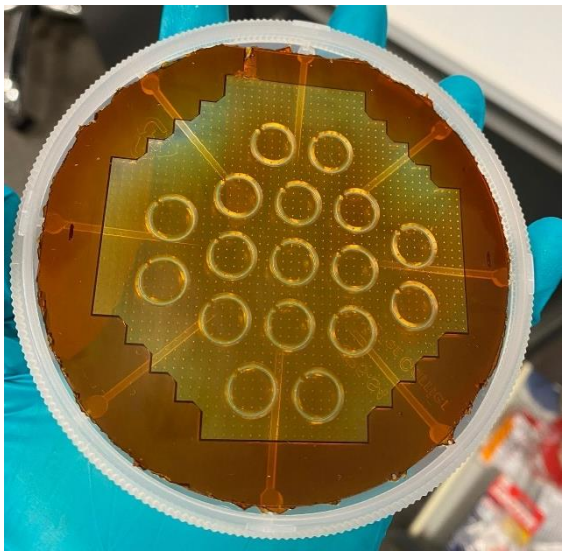

Figure 6. Wafer degassed and cured before metallization.

2.4. Metalization

Metallization is carried out by a third party.

2.5. *Passivation*

The microneedle arrays are coated with NOA68, using the coating includes 3 steps: 700 rpm for 10 seconds, 1500 rpm for 20 seconds, and 3000 rpm for 60 seconds. Simultaneously, it forms a thin, transparent film that adheres effectively to the surface, preventing signal interference. Additionally, its low viscosity facilitates excellent surface wetting, enhancing adhesion and coverage, even on irregular surfaces. The NOA-coated arrays require curing in a UV oven for 60 seconds.

2.6. Mounting

Reusable holders, printed with a 3D printer, are used for this purpose. Inside these holders, a cable is inserted and secured in a small opening in the 'head' area, and with tape to keep it in place. In the circular opening designed for the arrays, a double-sided adhesive tape is inserted, leaving the wire exposed, on which the back part of the array will rest.

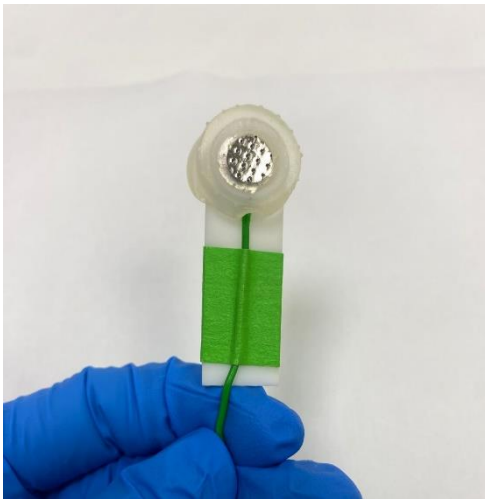

Figure 7. Mounted metallized arrays of microneedles.

2.7. Electrochemistry setup

An AUTOLAB Metrohm, potentiostat/galvanostat, is utilized for this purpose. A potentiostat is an electrochemical instrument that controls the potential difference (voltage) between the working electrode and the reference electrode while measuring the resulting current flow between the working electrode and the counter electrode (also known as the auxiliary electrode). The electrochemical system is placed inside the Faraday cage, provided with the AUTOLAB.

A three-electrode system is used, comprising the working, reference, and counter electrodes. In the initial phase of the work, the reference and the counter were commercially available electrodes, made of Ag/AgCl and platinum, respectively, while only the working electrode was made of platinum-metallized microneedles. Subsequently, all three electrodes were microneedle-based, with the working electrode being passivated platinum, the reference

electrode being non-passivated platinum, and the counter electrode being non-passivated gold. Depending on the ongoing experiment, the software was launched, and the data was recorded.

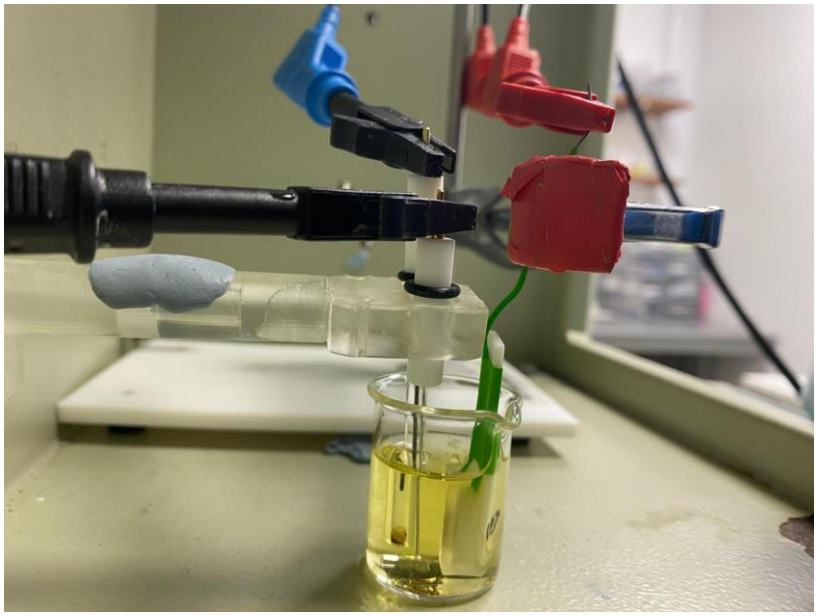

Figure 8. a) External electrochemistry set-up consisting of a microneedle-based working electrode, a commercial reference (Ag/AgCl) and counter (Platinum). The working electrode is mounted on a 3D-printed holder.

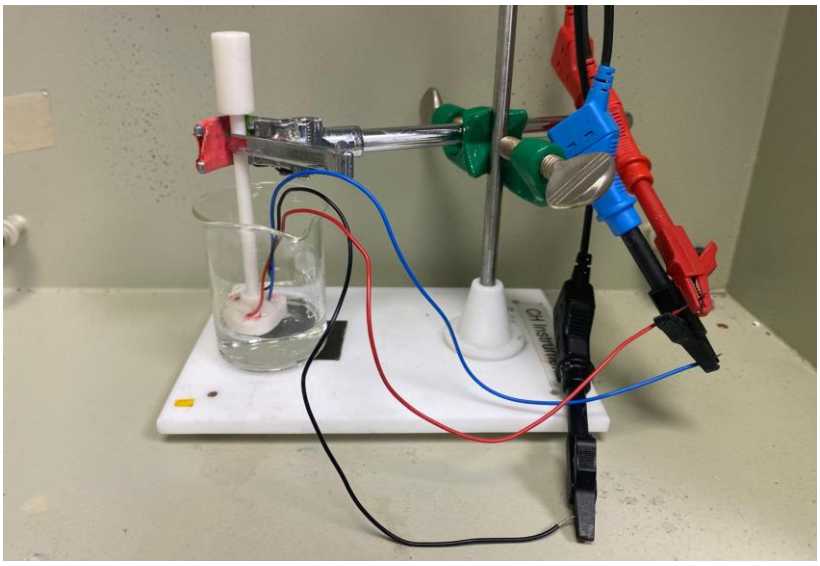

b) On-patch electrochemistry set-up, working, reference and counter were microneedle-based, platinum passivated, platinum non passivated and gold non passivated respectively. Electrodes mounted on a 3D-printed holder.

2.8. Microneedle Testing

Cleaning the sensors using CV ranging from -0.7 to +0.6 V or from 0 to +0.6 V at 50 mV/s was performed for the on-patch setup and external setup respectively. Electrodeposition of IrOx were performed using CV cycling the potential from -0.7 to +0.6 V for 20 cycles at a scan rate of 100 mV/s. Similarly, for the electrodeposition of PANI, CV was employed cycling the electrode potential over a range of values from -0.1 to +1.2 V for 10 cycles.

Amperometry was used to deposit PEDOT onto the MN array for 60 seconds, against an Ag/AgCl (RE) and Pt wire (CE).

For potassium detection, MN arrays were subjected to square wave voltammetry (SWV) by cycling the potential from -0.6 to +0.4 V with a step of 0.005 V, a modulation amplitude of 0.02 V, and a frequency of 25 Hz.

For pH measurements, the tests were conducted using open OCP measurements for 60 seconds, repeated 6 times with a 5-second interval between each measurement.

3. Results and Discussion

The microneedle-based sensors passivated were meticulously cleaned using FCA. Subsequent cyclic voltammetry (CV) revealed a cleaner and more well-defined curve, indicating the removal of surface contaminants and confirming the electrode's suitability for further modifications.

3.1. Potassium sensors

3.1.1. Characterization of the surface

In our study, sensors designed for potassium detection underwent surface modification utilizing PEDOT. Electrodeposition of PEDOT was accomplished using chronoamperometry for 30 seconds, ensuring a uniform and well-defined polymer layer on the sensor surface.

All the measurements for potassium sensors were made using the on-patch set-up.

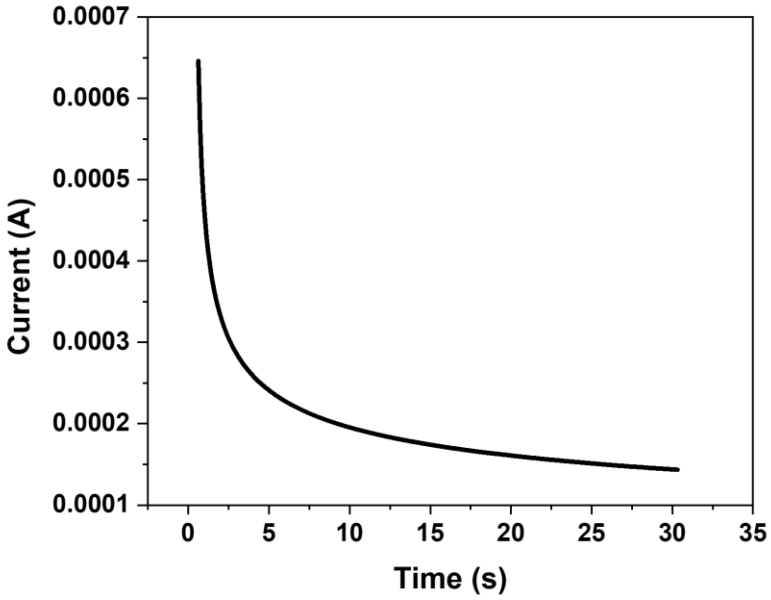

Figure 9. Chronoamperometry performed to electrodeposit PEDOT.

After the surface modification with PEDOT, an ion-selective membrane was applied onto the sensor surface.

As shown in Figure10, the surface modification using PEDOT significantly increased the recorded current, demonstrating the effectiveness of the conductive polymer. After the overnight application of the ISM, an additional change in the shape of the curve is observed. This alteration is attributed to the incorporation of the ISM, which influence the electrochemical behavior of the sensor, enhances the sensor's specificity by allowing selective permeation of potassium ions while minimizing interference from other ions, so the measured current is lower.[55]

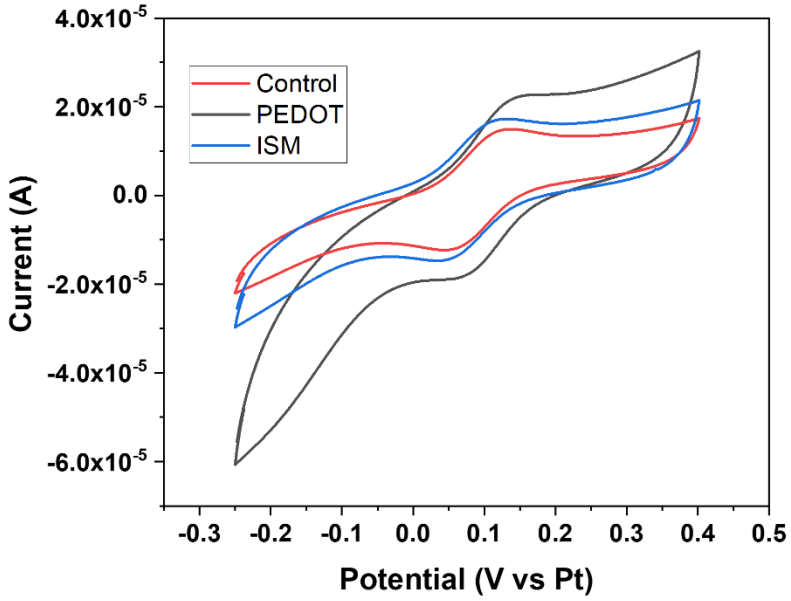

Figure 10. CV performed on the control (non-modified sensor), PEDOT-modified sensor and PEDOT-ISM-modified sensor.

3.1.2. Calibration

As shown in Figure 11, square wave voltammetry was performed in solutions with increasing concentrations of potassium. This resulted in a corresponding increase in current and a shift in the peak position, indicating a proportional relationship between these parameters, current and concentration. At higher concentrations of potassium ions, the sensor surface may become saturated. This saturation effect led to a disproportionately high current response because the available active sites on the sensor surface are fully occupied by the ions, resulting in a higher electrochemical reaction rate than anticipated.[51]

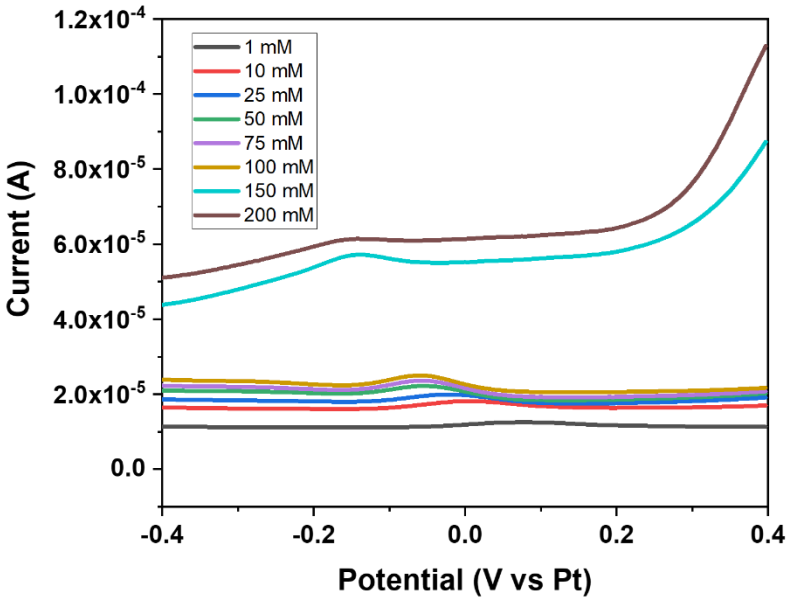

Figure 11. SWV performed on PEDOT-ISM-modified sensor in solution with increasing concentration of potassium ions.

The data obtained from the SWV, specifically the current values corresponding to the peak, were used to construct a calibration curve with a correlation coefficient of 0.992. Considering the logarithmic values of the dilution concentrations, the calibration curve was thus obtained.

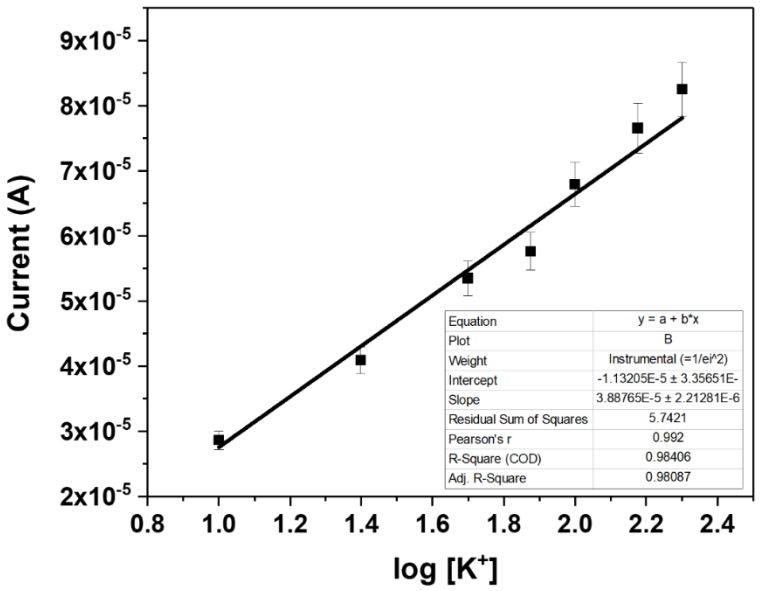

Figure 12. Calibration curve for potassium sensors.

The IUPAC's 1975 definition[58] defines the limit of detection (LOD) as the smallest concentration of an analyte that can be detected with reasonable certainty using a specific analytical method; so, it represents the lowest concentration at which an analytical procedure can reliably identify an analyte. The LOD obtained was of 1,49 mM covering the normal range of potassium concentration in human blood (approximately 3.5 to 5 mM)[41]: indicate that the biosensor is sensitive and capable of detecting amounts of potassium ions in a sample. While this LOD is lower compared to other studies[27], where LODs are often in the micromolar range, it is still within a clinically relevant range for detecting significant deviations in potassium levels.[41] This includes conditions like hyperkalemia, where serum potassium levels exceed the normal upper limit (above 5 mM). Thus, despite the higher LOD, the biosensor is suitable for practical clinical applications where precise detection of abnormal potassium levels is crucial.[41]

The formula to calculate the LOD for analytical methods is often expressed as:

$$LOD = 10^{3x(\frac{Standard\ deviation\ of\ the\ Blank}{Slope\ of\ the\ calibration\ curve})}$$

3.1.3. Interferences

An artificial interstitial fluid (ISF) was recreated to test the modified sensors, as a complex buffer that mimics the fluid in the body was made. Following the methodology of a study by Huijie Li et al.[28] their investigation demonstrated that the sensor exhibited a linear response to increasing potassium concentrations, indicating high sensitivity and accurate interpretation of rising potassium levels in skin ISF. Observing the graph, it was noted that the behavior remains quite consistent and coherent compared to the tests conducted with known concentration solutions. It suggests that the sensor is robust and not strongly influenced by the nature of the solvent used for dilution, other analytes did not interfere excessively. The measurements in artificial ISFs using calibrated sensors confirm the accurate measurements of physiological electrolytes in artificial ISFs.

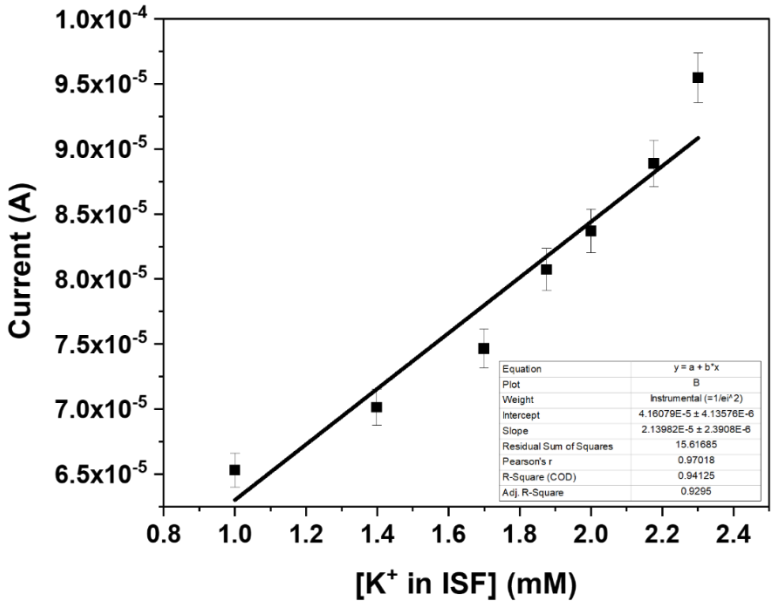

Figure 12. Calibration curve for potassium sensors obtained in solution with a higher concentration of potassium diluted with ISF.

The sensor's response was tested in various solutions containing potassium with sodium, calcium, and magnesium, respectively, to assess potential cross-reactivity or interference from these ions, which are commonly found in biological samples.

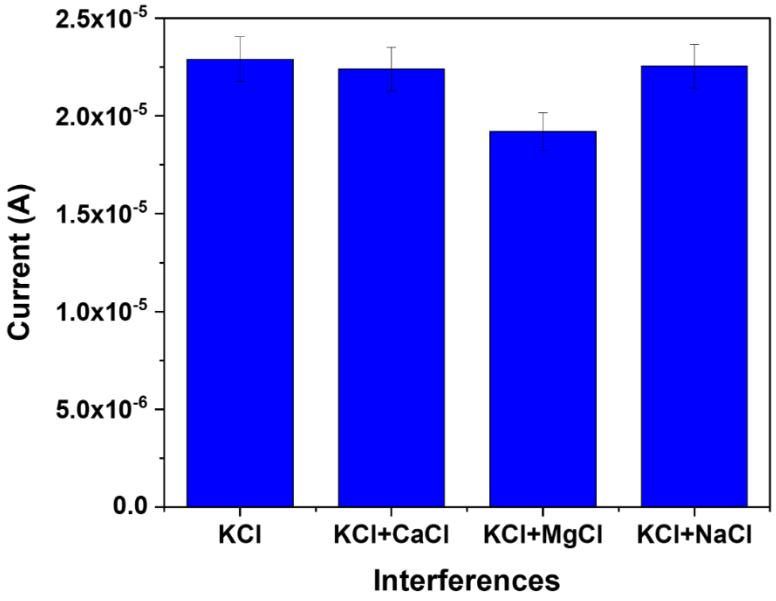

Figure 13. Bar graph representing the influence of different ions on the sensor's measurement.

During interference studies magnesium was identified as the analyte most affecting the detection of potassium, while calcium and sodium didn't show particular interferences, respectively of -16.10%, +2.19%, -1.55%. The higher interference from magnesium compared to sodium and calcium results from magnesium's higher charge density, stronger binding interactions, and greater impact on the electrochemical environment of the sensor. This makes it more competitive for binding sites and more disruptive to the sensor's ability to specifically detect potassium ions. Sodium and calcium, with their different charge densities and binding behaviors, do not interfere as significantly.[44] This finding highlights the importance of understanding potential cross-reactivity between analytes and optimizing sensor selectivity to ensure accurate and reliable measurements in complex biological samples, enhancing their suitability for practical applications.

Chen et al.[51] developed a sensor that the response can be adjusted by comparing the decrease in current against the initial baseline measurement. When measuring potassium, the sensor also encounters other ions, but their interference is minimal. The suppression or reduction in the sensor's signal caused by these other ions is less than 5%, indicating that their impact is negligible.

Table 4. Recorded current values in solutions containing different analytes and their corresponding interference percentages, relative to the KCl solution which represents 100%

SOLUTION	**CURRENT (µA)**	**PERCENTAGE *(%)***	**RESULT*ING* INTERFERENCE *(%)***
• *KCl*	22,90	100	0
• *KCl + NaCl*	22,55	98.45	-1,55
• *KCl + $MgCl_2$*	19,21	83.90	-16.10
• *KCl + $CaCl_2$*	22,40	102.19	+2.19

3.1.4. Negative control

This control helps to validate the sensor's ability to selectively detect the intended analyte in the presence of other compounds, ensuring the reliability and accuracy of the analytical results.

Comparing the current measured in the negative control with that obtained in the presence of the target analyte provides valuable insights into the sensor's performance. A lower current in the negative control compared to the analyte-containing samples (Figure 13) highlights the

sensor's high selectivity. This difference in current serves as a quantitative measure of the sensor's ability to distinguish between the target analyte and potential interferents, further confirming its suitability for specific analytical applications.[15]

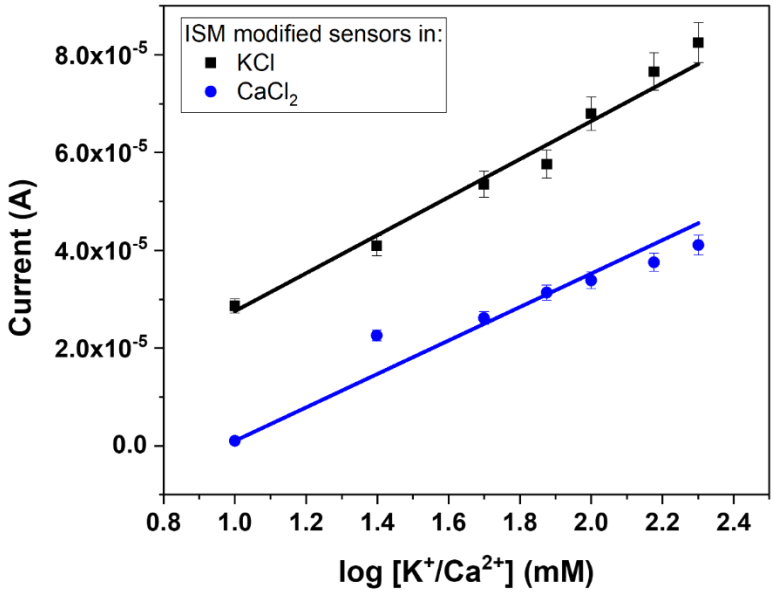

Figure 13. Calibration curve for potassium sensors (PEDOT-ISM-modified) in solution with increasing concentration of KCl and $CaCl_2$.

The sensors were additionally evaluated without any surface modification (Figure 14), relying solely on passivation, to emphasize the significance of employing an ion-selective membrane. This comparison underscores the pivotal role of the membrane in enhancing sensor performance by minimizing interference and improving selectivity.[55]

In this case, to assess the effectiveness of the superficial modification of the sensor, a t-test was performed to compare the current values obtained using cyclic voltammetry (CV) in a solution with the lowest concentration of the analyte for both unmodified and modified sensors. The results indicated a p-value of less than 0.05, demonstrating a statistically significant difference between the two groups. This analysis was conducted for sensors in this comparison: unmodified vs. PEDOT-ISM-modified. Also, in a study conducted by Shi et Al. on the surface modification of screen-printed carbon electrodes demonstrated significant improvements in sensor performance after superficial treatment. The t-test revealed a statistically significant difference in sensitivity between modified and unmodified electrodes, with the modified sensors showing enhanced sensitivity due to increased antibody adsorption sites created by the surface treatment.[59]

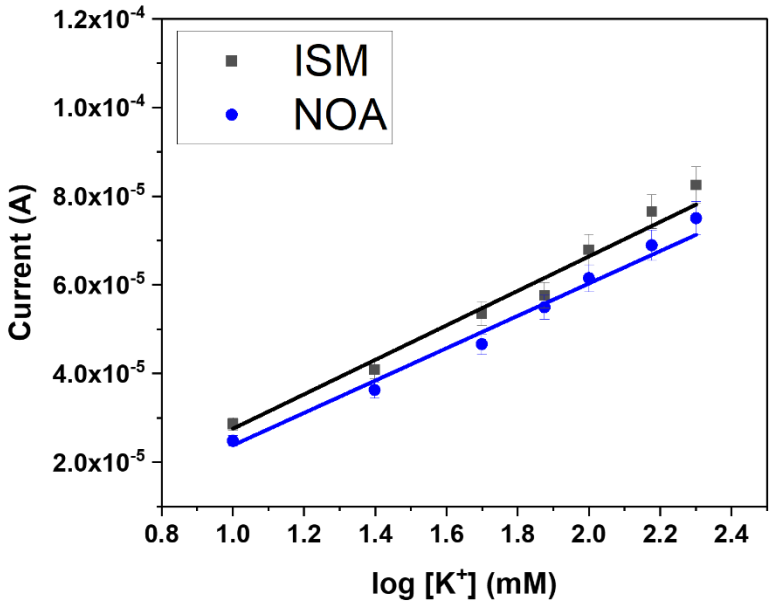

Figure 14. Calibration curve for potassium sensors without any surface modification (NOA) and PEDOT-ISM modified.

The sensors were evaluated on days 1, 7, 14, and 30 to assess their stability over time. As illustrated in Figure 15, there was a noticeable decline in sensitivity over the testing period, indicated by a decreasing slope of the calibration curve. Despite this high decline in sensitivity[14], the consistency of the sensors remained consistent, highlighting their reliability over extended periods. The correlation coefficient (R^2) serves as a measure of the calibration curve's reliability and can be used to assess the quality of the calibration process. The R^2 quantifies the degree of linear relationship between the sensor response and analyte concentration in a calibration curve, comparing the R^2 values of calibration curves obtained on different days can highlight the biosensor's consistency.[14] High R^2 values across different days suggest that the biosensor's performance is stable and is consistent.

On day 1, the R^2 value was 0.981; by day 7, it had decreased to 0.975. On day 14, it slightly increased to 0.995, but by day 30, it dropped further to 0.953. The observed stability loss in our biosensor, with reductions of 28.8%, 29.8%, and 35.3% on days 7, 14, and 30, respectively, could be due to factors related to ISM and their interaction with air. The degradation of stability over time could be due to the ISM's sensitivity to environmental conditions, including exposure to air, which may lead to changes in its properties and affect sensor performance.[55] In comparison, García-Guzman et al.[37] reported that their sensor retained 80% of its initial signal after 30 days, suggesting that their sensor's stability was less impacted by environmental factors. This discrepancy underscores the need to further investigate and address the stability of the ISM

and its interaction with the environment to improve long-term sensor performance and reduce the observed performance degradation.

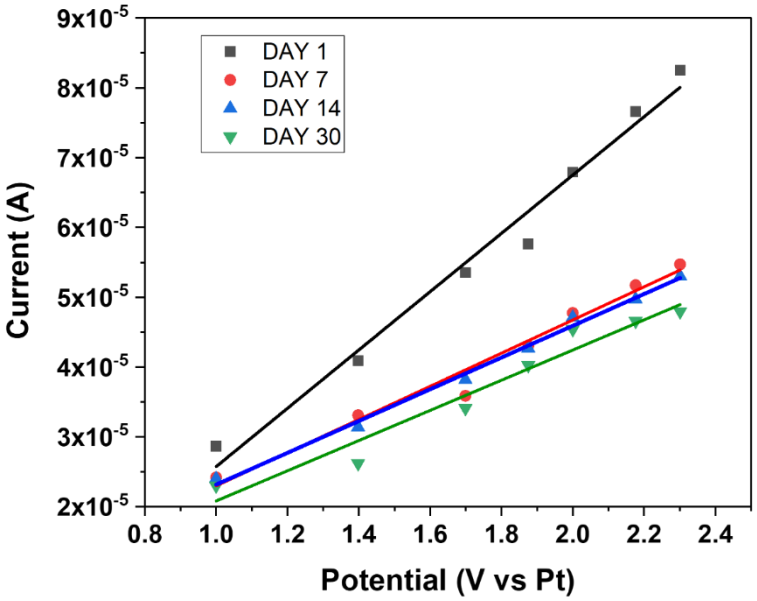

Figure 15. Calibration curve for potassium sensors from day 1 to 30.

Cyclic voltammetry (CV) was performed on unmodified sensors, PEDOT-modified sensors, and PEDOT-ISM-modified sensors, varying the scan rate and recording the anodic (Ipa) and cathodic (Ipc) peak currents. The coefficient of variation (CV) was assessed in all these cases to understand how the scan rate affects the measurements, noting that the smallest fluctuations occurred at a scan rate of 0.05 V/s. This value provides the most consistent and precise measurements, this suggests that the sensor's performance is most stable at this scan rate.

$$CV = \frac{Standard\ Deviation\ (A)}{Mean\ Current\ (A)} x\ 100$$

Table 5. Coefficient of variation calculated varying the scan rate from 0.01 to 0.2 V/s.

Scan Rate (V/s)	CV (%)
0.01	2.22 %
0.025	0.82 %
0.05	0.51 %
0.075	1.54 %
0.1	2.15 %
0.15	1.04 %
0.2	1.36 %

The electrochemically active area was calculated using the Randles-Sevcik equation. Here, *ip* represents the anodic and cathodic peak currents, *n* is the number of electrons transferred (1), *D* is the diffusion coefficient (2,32E-03 cm^2/s), *C* is the concentration of the electroactive species in solution (1E-06 mol/cm^3), and *v* is the scan rate (0.05 V/s). The active area was compared to the geometric area of the electrode, which was measured to be 0.0867 cm^2.

$$A = \frac{i_p}{2.69x10^5\, n^{\frac{3}{2}}\, C\, \sqrt{Dv}}$$

Table 6. Percentage of electrically active area of the microneedles relative to the anodic and cathodic peak current for the unmodified sensor, PEDOT-modified, PEDOT-ISM-modified

		Active Area (cm^2)	Aa/Ag	% Active Area
CONTROL	Ipc	0,12	1,43	42,50
	Ipa	0,12	1,35	34,99
PEDOT	Ipc	0,23	2,68	168,15
	Ipa	0,20	2,31	131,36
PEDOT-ISM	Ipc	0.31	3,58	258,29
	Ipa	0.28	3,19	218,62

It is evident from the table that the active area increases following surface modifications, indicating an enhancement in the sensing area, which likely improve the electrode's ability to facilitate electrochemical reactions. In the study of Chen et al.[51], to demonstrate that surface modification can significantly enhance the active area of electrodes, cyclic voltammetry (CV) was used to measure the active surface areas of both a bare gold electrode and a gold electrode modified with gold nanoparticles.

Assuming a specific charge, it was found that the modified gold electrode had a total active surface area 3 times higher than the bare gold electrode. These results underscore the significant impact of surface modification on increasing the active area of electrodes, which is crucial for improving the sensitivity and overall performance of biosensors. By enhancing the active surface area, the modified electrodes can provide a greater interface for electrochemical reactions, leading to better detection capabilities and more reliable sensor performance over time.

3.2. pH Sensors

3.2.1. Iridium Oxide modified sensors

3.2.1.1. Characterization of the surface

To ensure the selectivity of the biosensor, surface modifications were performed using IrOx and PANI; they exhibit a particular affinity for pH sensing due to their unique chemical properties and electrochemical capabilities.

IrOx deposition was achieved through 20 cycles of CV at a scan rate of 0.1 V/s. The application of IrOx coating significantly enhanced the electrical conductivity of the electrode, leading to a pronounced increase in current responsiveness. This observed behavior is depicted in Figure 17, where the CV curve distinctly illustrates the heightened current responsiveness attributable to the IrOx coating.

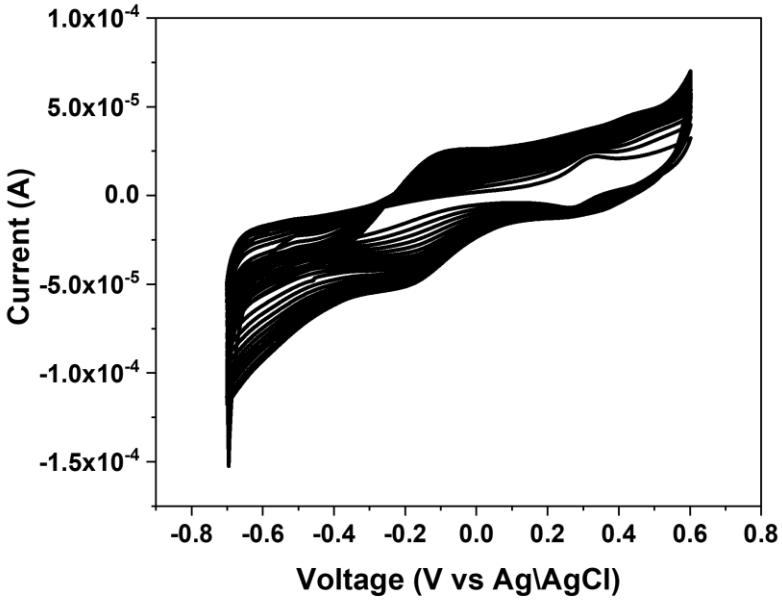

Figure 16. 20 cycles of CV performed to electrodeposit IrOx.

The CV analysis reveals significant improvements in the electrochemical performance of the platinum electrode following surface modification with iridium oxide. As Salimi et al.[60] affirm in their study that the currents on the scans consecutive to the modification, increase indicating formation of an electroactive deposit on the electrode surface.

The cathodic peak potential shifted from 0.121 V (6.58 µA) in the control electrode to 0.136 V (18.2 µA) in the modified electrode. Similarly, the anodic peak potential shifted from 0.060 V (-3.90 µA) to 0.045 V (-14.3 µA) (Figure 16). These shifts and the substantial increase in peak currents indicate that the iridium oxide modification effectively enhances the active surface area, improving electron transfer kinetics and overall sensitivity. These results confirm that surface modification with iridium oxide significantly enhances the electrode's performance, making it more effective for applications requiring high sensitivity and reliable detection.

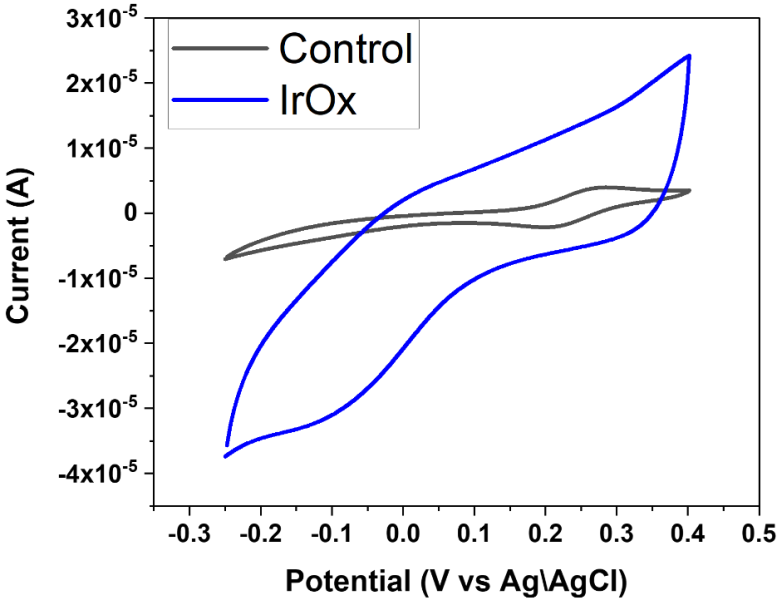

Figure 17. CV performed on the control (non-modified sensor) and on the IrOx-modified sensor.

3.2.1.2. Calibration curve

During the modification of electrodes with IrOx, several approaches were attempted to optimize the deposition process. These included varying the deposition solutions and adjusting the number of cycles used for the electrochemical deposition. Despite these efforts, the results were not as satisfactory as anticipated.

The tests involved submerging the sensors in solutions with pH 3, 5, 7, and 9 and measuring OCP. The coefficient of determination obtained was 0.94, indicating a good but not perfect correlation between the experimental measurements and the expected values.[61] This suggests that while the surface modification with IrOx improved the sensor performance to some extent, it did not achieve the high level of enhancement observed with other modifications. IrOx deposition can be highly sensitive to the electrochemical environment and parameters. Even minor variations in these conditions could lead to inconsistent surface coverage and performance.[58]

The observed slope of -33 mV/pH (Figure 18), which deviates from the theoretical Nernstian response, can be attributed to several factors. Primarily, it appears that the iridium oxide layer didn't enough facilitate a fully Nernstian response in laboratory conditions. The microneedle structure presents a complex geometry that could affect the uniformity of the IrOx film during electrodeposition. Non-uniform deposition can create areas with different electrochemical properties, causing deviations from ideal behavior.[27] Another reason could be the chemical nature of the surface on which IrOx is deposited impacts the film's adhesion and stability. If the surfaces have variable chemical characteristics, this could affect how well the film adheres. Poor adherence can lead to delamination or degradation of the film over time.[56] Thid could be attributed to the passivation method that is hand-operated.

Despite the challenges, the modification with IrOx result in a measurable improvement, as indicated by the R^2 value. This suggests potential for further optimization and highlights the importance of continued research into the precise conditions needed for effective IrOx deposition. The modified electrode exhibited a responsive behavior to pH changes, indicating successful surface modification and sensitivity improvement. This responsiveness, while not ideal, is a positive outcome as it demonstrates the potential for further optimization.

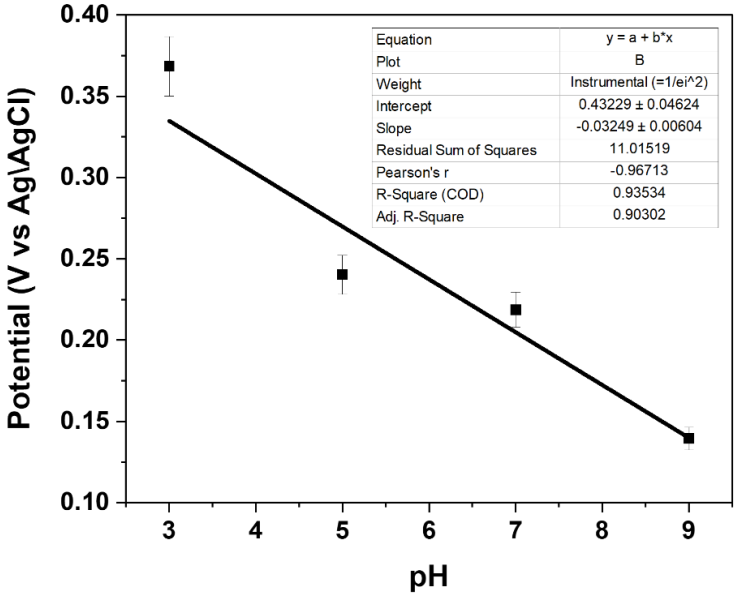

Figure 18. Calibration curve for pH sensors modified with IrOx, tested with an external set-up.

Tests were performed using both external and on-patch setups, allowing for evaluation under different conditions that simulate practical applications and controlled environments.

Transitioning to a system of three microneedle-based electrodes introduces several factors that contribute to changes in the calibration curve. Microneedle electrodes, with their reduced surface area and potential mechanical instability, alter the electrochemical behavior compared to commercial electrodes. The geometry and surface chemistry of microneedle electrodes, especially when modified with IrOx coatings, necessitate recalibration to account for differences in sensitivity and selectivity.

The observed positive slope in pH measurements when switching from an external setup, which employs a commercial Ag/AgCl reference electrode, to an internal setup, utilizing a platinum microneedle as the reference electrode, can be attributed to differences in the stability and behavior of the reference electrodes. The commercial Ag/AgCl reference electrode is composed of a silver wire coated with silver chloride in contact with a filling solution, where the potential depends solely on the chloride concentration. Since this concentration is fixed, the electrode potential remains stable and reliable, providing a consistent basis for accurate pH measurements.[3] In contrast, the platinum microneedle's potential could vary based on the surrounding solution and surface condition. This variability can be influenced by several factors such as local ion concentrations, interactions with the IrOx surface, and environmental changes like pH fluctuations and temperature variations. As a result, the platinum microneedle does not

provide the same stable reference potential as the Ag/AgCl electrode, leading to the positive slope observed in the calibration curve. This reflects the influence of the added complexities and variabilities inherent in the internal setup, highlighting the need for further optimization of the reference electrode design to achieve more consistent and reliable pH measurements.[26]

Despite this deviation, the sensor may still provide reliable pH measurements under these conditions with a coefficient of variation of 0.95.

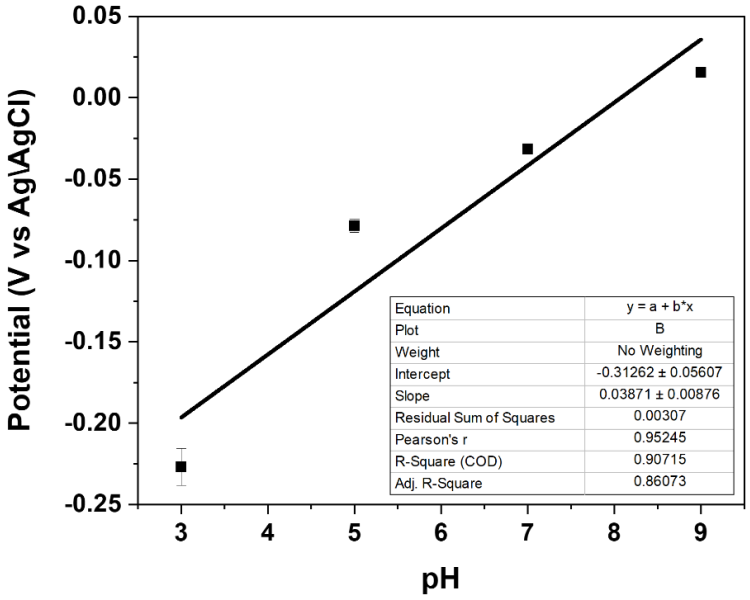

Figure 19. Calibration curve for pH sensors modified with IrOx tested with an on-patch set-up.

3.2.2. PANI modified sensors

3.2.2.1. Characterization of the surface

The performance of IrOx sensors can vary, particularly in terms of sensitivity and stability over time. While IrOx offers good selectivity for pH, its limitations may prompt us to explore alternative materials for pH sensing. Unlike IrOx, PANI demonstrates notable advantages such as higher sensitivity, enhanced stability, and improved selectivity for pH sensing. PANI-modified sensors have shown superior performance and reliability compared to IrOx. [62]

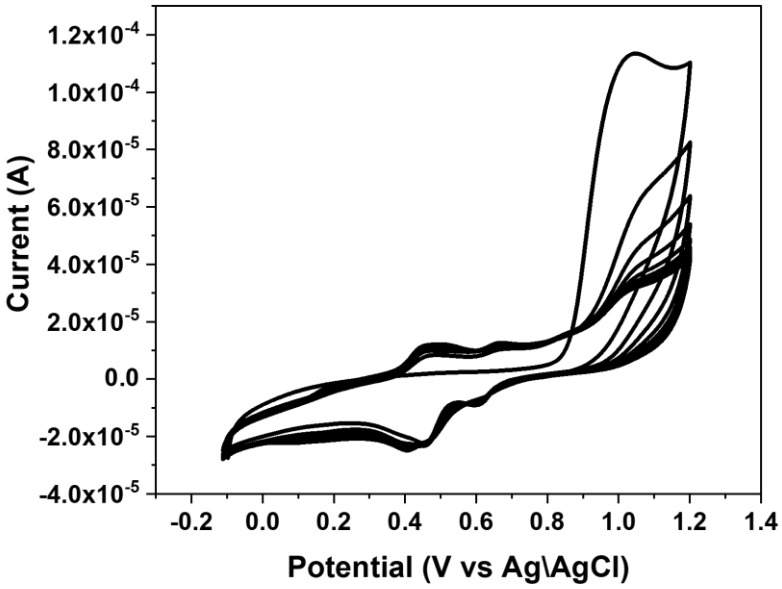

Figure 10. 10 cycles of CV performed to electrodeposit PANI.

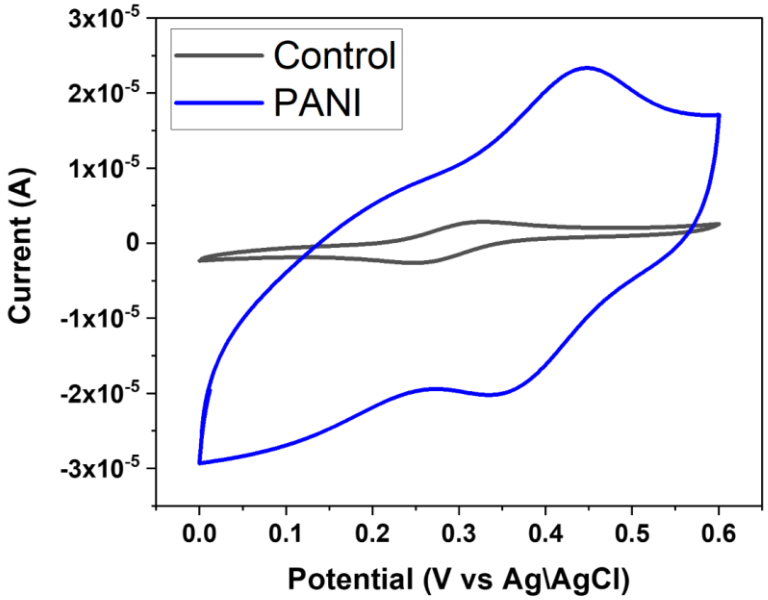

Figure 11. CV performed on the control (non-modified sensor) and on the PANI-modified sensor.

Figure 20 illustrates the deposition process of polyaniline (PANI) through 10 cycles of CV scanning. During the scanning cycles, clear oxidation and reduction peaks are visible. The two oxidation peaks correspond to the formation of two different oxidized states of polyaniline, while the two reduction peaks indicate the reduction of these oxidized states during the

polymerization process; the presence of well-defined peaks suggests controlled and reproducible deposition of the polymer material. [57]

As shown in Figure 21, comparing the control with the PANI-deposited sample using CV, a noticeable increase in current is observed, indicating the enhanced conductivity conferred by the deposition of PANI. In the study of Gojeh et al.[63] the voltammetric response of both bare and PANI-modified electrodes was recorded and compared. They demonstrate the overlay of the voltammograms obtained at these three electrodes. A significant increase in current response was observed for the PANI-modified electrode compared to the bare electrode. This enhancement in current indicates a higher electrochemical activity upon modification.

The increased current response can be attributed to the increased electroactive surface area provided by the PANI modification. The porous structure and high surface area of PANI introduce additional active sites and facilitate greater interaction with the electrolyte, resulting in a higher current response. Moreover, PANI's conductive nature improves charge transfer properties, reducing resistance and enhancing the overall efficiency of electrochemical reactions.[57]

3.2.2.2. Calibration curve

The calibration curve derived from samples modified with PANI exhibits a slope more closely aligned with that of the Nernst equation, of -40 mV/pH, with a coefficient of determination of 0.958. Consequently, the results surpass those obtained with sensors modified by IrOx.

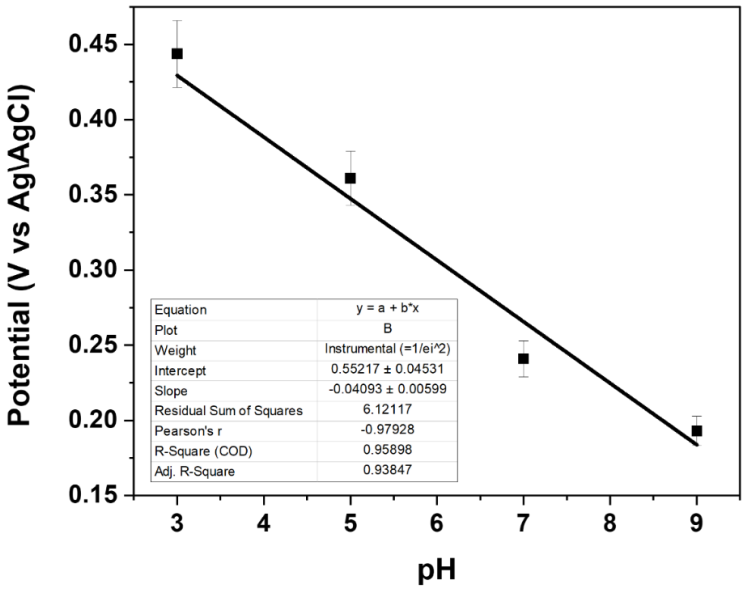

Figure 22. Calibration curve for pH sensors modified with PANI tested with an external set-up.

However, PANI-modified sensors were exclusively tested using the external set-up, indicating a potential area for further exploration and refinement.

The performance of PANI-modified sensor was tested for pH testing over a period of 7 days (Figure 23). Notably, the sensor exhibited the same slope in its calibration curve after 7 days, indicating stable sensitivity and selectivity for pH measurements. This consistency suggests that the fundamental interaction of PANI with hydrogen ions remained intact, maintaining the sensor's accuracy.[57]

However, a significant decrease in the registered potential was observed. This reduction in current, despite the consistent slope, indicates a decline in the overall electrochemical activity of the sensor. PANI is known to undergo physical and chemical changes over time, such as oxidative degradation and changes in its doping state, which can reduce its conductivity. Environmental exposure and morphological changes like swelling or cracking can all contribute to a decrease in current by reducing the number of active sites available for protonation and altering the electrode surface area.[34]

These findings highlight the importance of regular calibration and potential rejuvenation of the PANI layer to maintain optimal sensor performance. Future improvements could focus on enhancing the stability of PANI through optimized synthesis, protective coatings, or developing new composite materials to ensure the longevity and reliability of PANI-modified sensors for pH measurement.

The sensitivity decreased by 38.3% after 7 days, and the coefficient of determination dropped to 0.947.

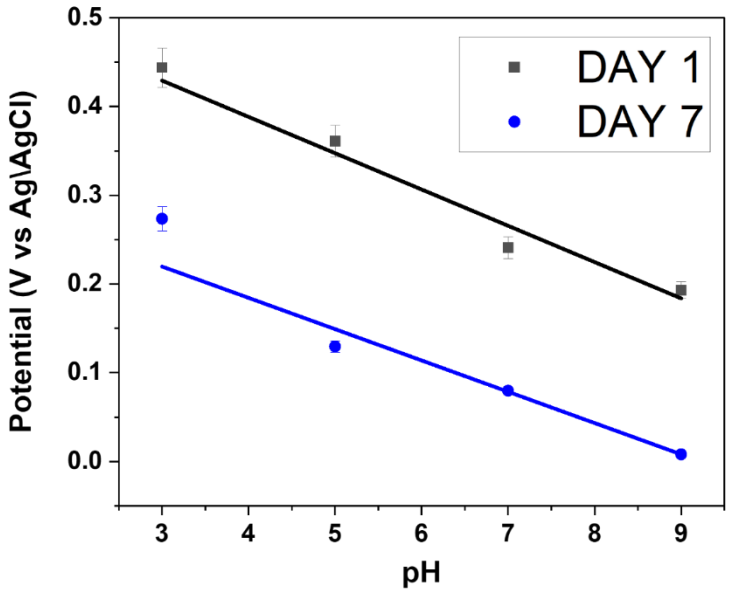

Figure 23. XXX

3.2.2.3. Negative control

Negative control test was conducted to highlight the improvement in sensitivity achieved by the deposition of PANI compared to samples without any surface modification. This behavior is clearly shown in Figure 24, where the registered potential significantly increases with the PANI-modified sensors, demonstrating their enhanced performance. Higher potential response at equivalent analyte concentration indicates improved sensitivity, this suggests that the PANI-modified sensor produced a stronger signal for the same analyte concentration. The slope for the PANI-modified sensors was -43.6 mV/pH, for the non-passivated sensors was -19.6 mV/pH, indicating a big loss of sensitivity, around 45%.

Supporting experimental findings, literature[63] indicates that pH fluctuations on the surface of the PANI sensor lead to corresponding increases or decreases in ion mobility, resulting in changes in the sensor's resistance. The resistance of the PANI membrane varies when contacting analytes with different pH, leading to changes in the output voltage.

This mechanism is consistent with our observations, where the PANI-modified sensor exhibited a higher current response and greater sensitivity to pH changes compared to the bare sensor. The enhanced performance of the PANI-modified sensor can be attributed to PANI's ability to alter its resistance based on ion mobility and pH fluctuations, ensuring high sensitivity and accurate pH measurement.

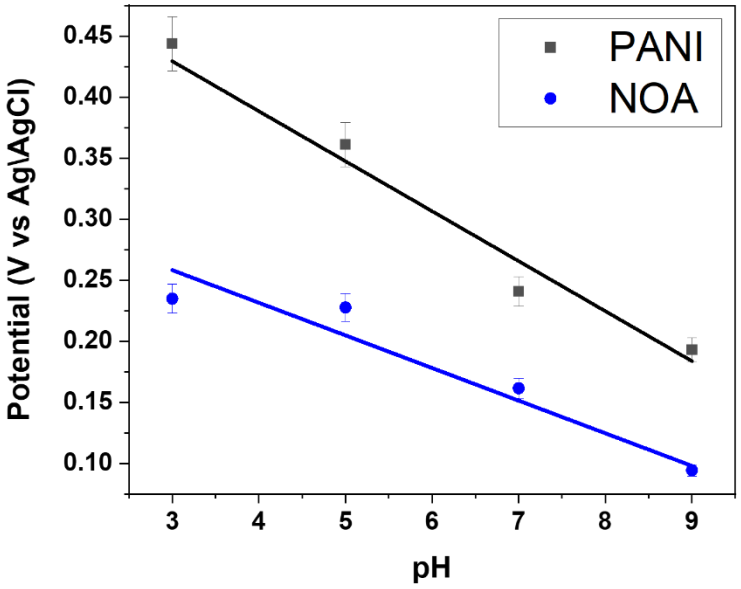

Figure 24. Calibration curve for pH sensors without any surface modification and PANI-modified.

3.2.2.4. Interferences

This study aimed to evaluate the influence of common ions present in the ISF on the sensor's performance. The calibration curve obtained in the ISF displayed a coefficient of determination (R^2) of 0.9, indicating a reasonably good correlation between the experimental measurements and the expected values (Figure 25). However, the slope of the calibration curve was -15.2 mV/pH, significantly deviating from the theoretical value predicted by the Nernst equation.

The deviation from the theoretical slope can be attributed to several factors. Common ions present in ISF can interfere with the pH measurement, altering the electrochemical response of the sensor. This interference may affect the ion-selective properties of the electrode and the equilibrium of the electrode reaction, leading to a reduced sensitivity and deviation from the ideal Nernstian behavior. The observed slope is lower than the expected -59 mV/pH, reflecting the impact of these ionic interferences. This finding is consistent with literature that reports similar deviations in pH sensors tested in complex media. For instance, Smith et al. observed slopes ranging from -20 to -30 mV/pH in artificial interstitial fluids, attributed to ion interference and matrix effects.[64]

Despite these challenges, the high R^2 value in this study suggests that the sensor still maintains a good correlation between the measured potential and pH, indicating its reliability even in the presence of interfering ions. To enhance sensor performance in complex environments, future work should focus on optimizing sensor design and calibration methods to mitigate the effects of ionic interference and improve sensitivity.

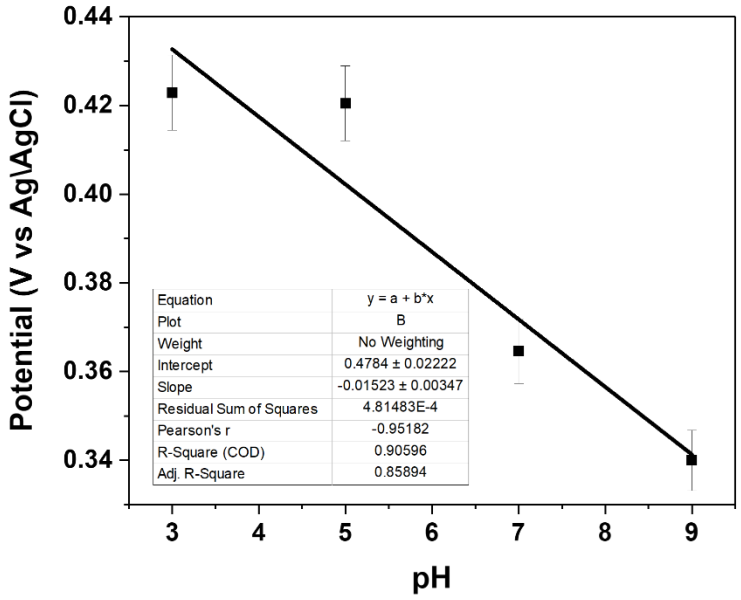

Figure 25. Calibration curve for pH sensors PANI-modified tested in artificial ISF.

An interference study was carried out to evaluate the sensor's response to common ions present in biological fluids. Four solutions were prepared: one with only the buffer and three others with the buffer supplemented with KCl, NaCl, and $MgCl_2$, respectively (Figure 26). All solutions were maintained at pH 5 to ensure a consistent pH environment. The response in the KCl solution was slightly higher than the baseline, indicating that potassium ions have a minimal impact on the sensor's accuracy for pH measurement at this concentration. The significant decrease in the sensor response in presence of sodium ions suggests a notable interference effect, as sodium ions may compete with hydrogen ions at the sensor surface, reducing pH measurement accuracy. The potassium ion has a larger ionic radius compared to the sodium ion. This is because potassium is located lower in the periodic table than sodium, meaning it has a greater number of energy levels and thus a larger ionic radius.[11] Regarding PANI, the lower tendency of potassium to form strong bonds with the functional groups of PANI can be attributed to its larger size and lower charge density compared to sodium. Smaller ions with higher charge density, such as sodium, tend to form stronger bonds with functional groups. Sodium, with its relatively small ionic radius, has a strong capacity to bind with the functional groups present on the surface of PANI. This interaction can compete with the protonation of PANI by H^+ ions, reducing the sensor's sensitivity and altering the open-circuit potential.[55]

Magnesium ions exhibited the greatest interference, with the sensor response dropping to 85.42%. The divalent nature of magnesium ions likely causes a more significant interaction at the sensor surface, further compromising the sensor's ability to accurately measure pH.

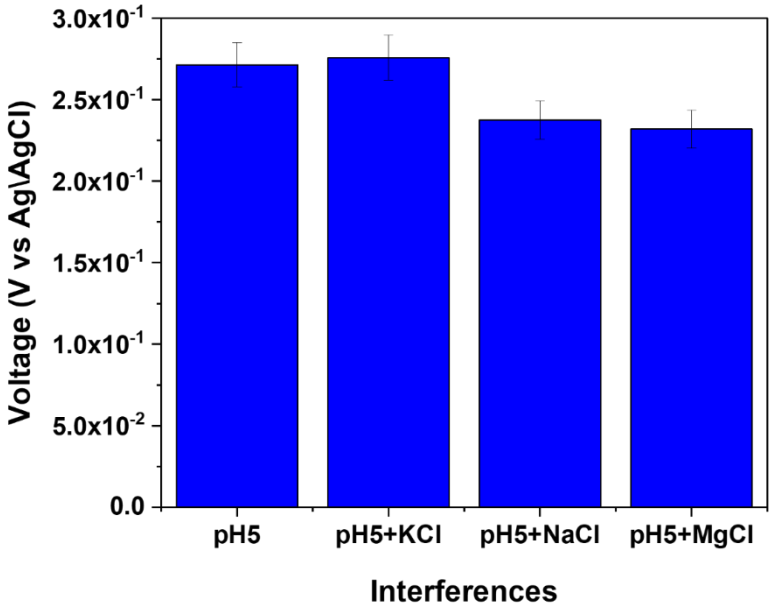

Figure 26. Bar graph representing the influence of different ions on the sensor's measurement.

Table 7. Recorded current values in solutions containing different analytes and their corresponding interference percentages, relative to the buffer solution which represents 100%

SOLUTION	**Open Circuit Potential (V)**	**PERCENTAGE *(%)***	**RESULT*ING* INTERFERENCE *(%)***
Buffer Solution (pH5)	0,27	100	0
Buffer + KCl	0,28	101,6	+1,60
Buffer + NaCl	0,24	87,54	-12,46
Buffer + $MgCl_2$	0,23	85,42	-14,58

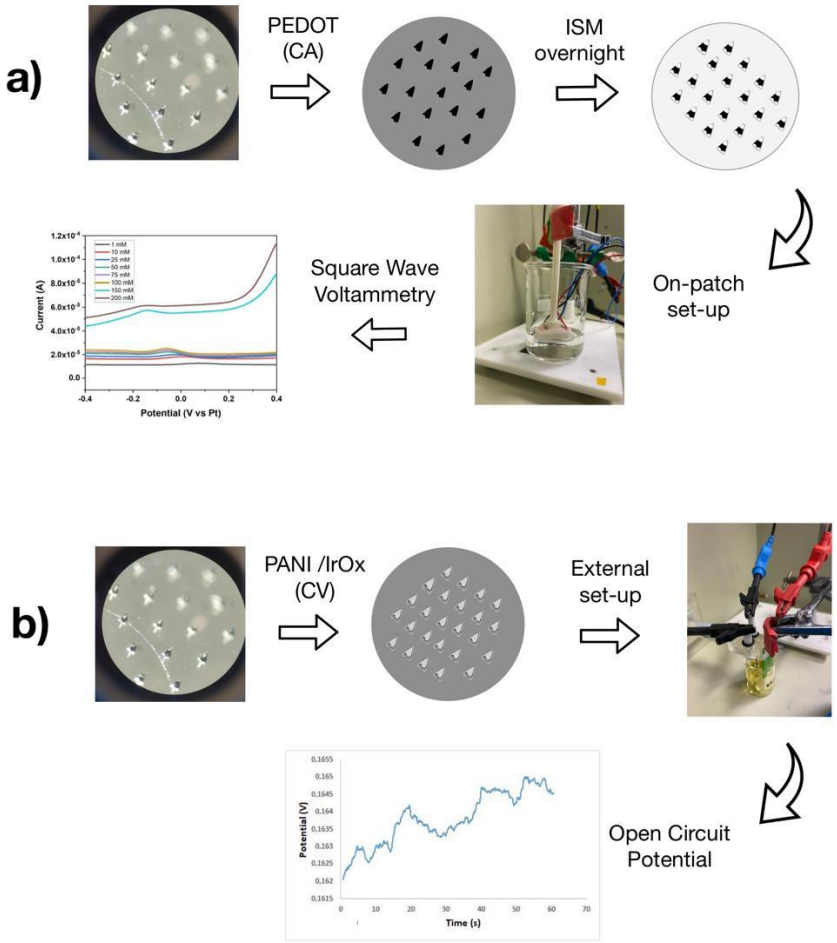

Figure 27. a) Schematic representation of potassium PEDOT-ISM-modified sensor tested with an on-patch set-up with SWV to detect different concentration of K+. b) Schematic representation of pH sensor PANI/IrOx-modified sensor tested with an external set-up with OCP to detect different pH.

3.3. Multiplexed sensor for detection of different parameters

In the laboratory, new software was developed and implemented to test multiple sensors simultaneously, specifically for detecting potassium and pH using SWV and OCP techniques. To facilitate this multiparametric detection, a specialized holder with four microneedle-based electrodes was designed and fabricated. This holder accommodated two working electrodes, one for pH and one for potassium, along with the reference and counter electrodes within the same system.

These sensors were connected to an integrated circuit, which interfaced with the software, allowing for control and measurement of the different analytes. While several challenges were encountered during the implementation phase, such as ensuring compatibility and stability of the system, this innovative approach facilitated the simultaneous detection of multiple analytes, enhancing the efficiency and effectiveness of point-of-care diagnostics.

The development of this multiparametric sensor system demonstrated the feasibility of real-time, on-site monitoring and highlighted its potential for a wide range of applications, including healthcare, environmental monitoring, and sports science. By providing a portable and reliable solution for the concurrent detection of potassium and pH levels, this technology could represent a significant step toward more comprehensive and versatile diagnostic tools.

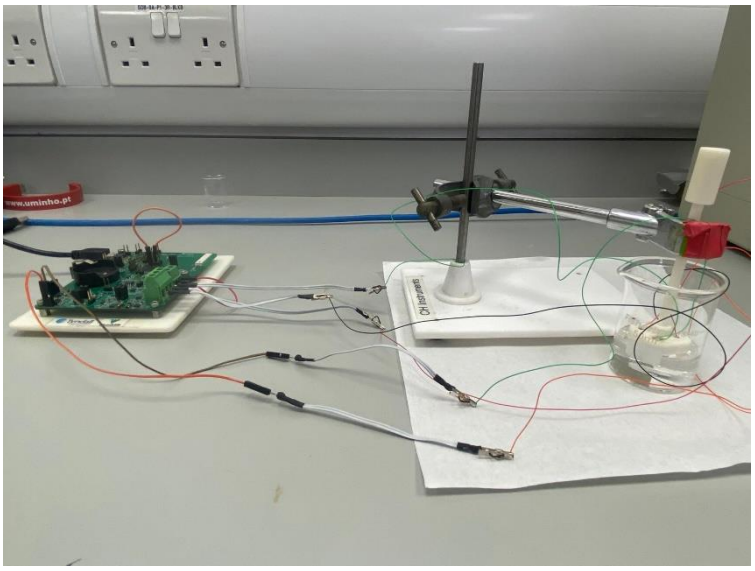

Figure 28. On-patch electrochemistry set-up. Reference, counter and 2 working electrodes mounted on a 3D-printed holder. Electrodes connected to an integrated circuit, connected to a software.

4. Conclusion

The results highlight the potential for real-time ion monitoring of potassium and pH. The sensors were fabricated using NOA passivation, which, while effective, could benefit from improvements due to the manual application process that can result in non-homogeneous surface coverage. Enhancing the passivation technique would likely improve the consistency and reliability of the sensors.

The study for potassium ion detection is more advanced, particularly with the use of the on-patch setup. This setup improves the sensor's applicability and enhances the concept of point-of-care diagnostics, a primary aim of this research. The calibration curve for potassium detection presented challenges in terms of sensitivity, although it demonstrated satisfactory linearity. Further optimization could improve the sensitivity, thereby enhancing the sensor's overall performance.

Interference studies for both potassium and pH sensors confirmed the biosensors' selectivity, indicating that these sensors can detect the target ions even in the presence of potential

interfering substances. This selectivity is crucial for reliable real-time monitoring in complex biological fluids like interstitial fluid.

The development of these microneedle biosensors aligns with the broader goals of point-of-care diagnostics, remote monitoring, and early disease detection. The microneedle format provides a minimally invasive method for continuous monitoring, making it suitable for various applications in healthcare and sports science. The compatibility of these sensors with current data collection and transmission technologies allows for real-time data sharing and remote monitoring, facilitating prompt medical interventions.

Moreover, the potential for multiplexed parameter sensing was explored by testing new software capable of simultaneously detecting potassium and pH. This advancement brings us closer to the goal of creating a comprehensive monitoring tool that can provide valuable health insights and support better patient outcomes.

Further optimization and validation are necessary to fully realize these results and their potential and integrate them into clinical practice. The creation of such advanced, user-friendly biosensors represents a significant step toward improving the precision and accessibility of ion detection in interstitial fluid, ultimately contributing to better healthcare outcomes and a deeper understanding of physiological processes.

4.1. Future prospectives

An essential approach for enhancing the performance and longevity of these sensors involves the development of innovative passivation materials. Current passivation techniques, such as NOA, have shown effectiveness but are limited by manual application, leading to potential inconsistencies in surface coverage. Exploring advanced passivation materials could offer higher chemical inertness, increased durability, and superior protection. These improvements would enable the sensors to function more reliably under a broader range of conditions, ultimately enhancing their performance and applicability in settings.

A significant advancement in sensor technology is the development of sensors capable of detecting multiple ions simultaneously. Implementing software capable of multiplexed detection will allow the integration of several receptors or detecting components, each selective for a different ion, into a single sensor unit. This innovation would enable the concurrent monitoring of various ions in a single test, optimizing time and resources while providing more comprehensive and reliable data. The creation of such multiplex sensors is a promising step toward more efficient and effective point-of-care diagnostics, facilitating the rapid and precise detection of multiple analytes to support better healthcare outcomes.

These enhancements will support the sensor's practical applicability, particularly in point-of-care diagnostics and remote monitoring scenarios. By providing accurate, real-time data on multiple analytes, biosensors will contribute to early diagnosis and timely medical interventions, ultimately improving patient care.

The continued development and optimization of these technologies will pave the way for their seamless incorporation into clinical practice, offering a robust foundation for future healthcare innovations.

Bibliography

(1) Utkarsh Chadha, Preetam Bhardwaj, Rushali Agarwal, Priyanshi Rawat, Rishika Agarwal, Ishi Gupta, Mahek Panjwani, Shambhavi Singh, Chirag Ahuja, Senthil Kumaran Selvaraj, Murali Banavoth, Prashant Sonar, Badrish Badoni, A. C. Recent Progress and Growth in Biosensors Technology: A Critical Review. **2022**.

(2) D R Thévenot, K Toth, R A Durst, G. S. W. Electrochemical Biosensors: Recommended Definitions and Classification. **1999**.

(3) Principles, D.; Ramesh, M.; Janani, R.; Deepa, C.; Rajeshkumar, L. Nanotechnology-Enabled Biosensors : A Review of Fundamentals ,. **2023**, 1–32.

(4) Parvin Samadi Pakchin a b, Sattar Akbari Nakhjavani b c, Reza Saber a, Hossein Ghanbari a, Y. O. Recent Advances in Simultaneous Electrochemical Multi-Analyte Sensing Platforms. **2017**.

(5) Mehrotra, P. Biosensors and Their Applications - A Review. *J. Oral Biol. Craniofacial Res.* **2016**, *6* (2), 153–159. https://doi.org/10.1016/j.jobcr.2015.12.002.

(6) Newman, J. D.; Setford, S. J. Enzymatic Biosensors. *Mol. Biotechnol.* **2006**, *32* (3), 249–268. https://doi.org/10.1385/MB:32:3:249.

(7) Li, Y. C. E.; Chi Lee, I. The Current Trends of Biosensors in Tissue Engineering. *Biosensors*

2020, *10* (8). https://doi.org/10.3390/bios10080088.

(8) Miroslav Pohanka. Overview of Piezoelectric Biosensors, Immunosensors and DNA Sensors and Their Applications. **2018**.

(9) Kumaran Ramanathan, B. D. Principles and Applications of Thermal Biosensors. **2001**.

(10) Kumar, A.; Mittal, S.; Das, M.; Saharia, A. Optical Biosensors : A Decade in Review. *Alexandria Eng. J.* **2023**, *67*, 673–691. https://doi.org/10.1016/j.aej.2022.12.040.

(11) Ahmed, S.; Shaikh, N.; Pathak, N.; Sonawane, A.; Pandey, V.; Maratkar, S. Chapter 3 - An Overview of Sensitivity and Selectivity of Biosensors for Environmental Applications; Kaur Brar, S., Hegde, K., Pachapur Techniques and Protocols for Monitoring Environmental Contaminants, V. L. B. T.-T., Eds.; Elsevier, 2019; pp 53–73. https://doi.org/https://doi.org/10.1016/B978-0-12-814679-8.00003-0.

(12) Malik, S.; Singh, J.; Goyat, R.; Saharan, Y.; Ameen, S.; Baskoutas, S. Heliyon Nanomaterials-Based Biosensor and Their Applications : A Review. *Heliyon* **2023**, *9* (9), e19929. https://doi.org/10.1016/j.heliyon.2023.e19929.

(13) Varnakavi. Naresh, N. L. A Review on Biosensors and Recent Development of Nanostructured Materials-Enabled Biosensors. **2021**.

(14) Chen, L.; Wang, E.; Tai, C.; Chiu, Y.; Li, C.; Lin, Y.; Lee, T.; Huang, C.; Chen, J.; Chen, L. Biosensors and Bioelectronics Improving the Reproducibility , Accuracy , and Stability of an Electrochemical Biosensor Platform for Point-of-Care Use. *Biosens. Bioelectron.* **2020**, *155* (September 2019), 112111. https://doi.org/10.1016/j.bios.2020.112111.

(15) Saputra, H. A. Electrochemical Sensors: Basic Principles, Engineering, and State of the Art. *Monatshefte fur Chemie* **2023**, *154* (10), 1083–1100. https://doi.org/10.1007/s00706-023-03113-z.

(16) Sharma, A.; Badea, M.; Tiwari, S.; Marty, J. L. Wearable Biosensors: An Alternative and Practical Approach in Healthcare and Disease Monitoring. *Molecules* **2021**, *26* (3), 1–32. https://doi.org/10.3390/molecules26030748.

(17) Lubken, R. M.; de Jong, A. M.; Prins, M. W. J. Real-Time Monitoring of Biomolecules: Dynamic Response Limits of Affinity-Based Sensors. *ACS Sensors* **2022**, *7* (1), 286–295. https://doi.org/10.1021/acssensors.1c02307.

(18) Ankur M. Kumar, K. K. Biomedical Applications of Bioelectrochemical Sensors. **2022**.

(19) Wang, Z.; Liu, N.; Ma, Z. Platinum Porous Nanoparticles Hybrid with Metal Ions as Probes for Simultaneous Detection of Multiplex Cancer Biomarkers. *Biosens. Bioelectron.* **2014**, *53*, 324–329. https://doi.org/10.1016/j.bios.2013.10.009.

(20) Shimaa Eissa, M. Z. Ultrasensitive Peptide-Based Multiplexed Electrochemical Biosensor for the Simultaneous Detection of Listeria Monocytogenes and Staphylococcus Aureus. **2020**.

(21) Kashefi-Kheyrabadi, L.; Nguyen, H. V.; Go, A.; Baek, C.; Jang, N.; Lee, J. M.; Cho, N. H.; Min, J.; Lee, M. H. Rapid, Multiplexed, and Nucleic Acid Amplification-Free Detection of SARS-CoV-2 RNA Using an Electrochemical Biosensor. *Biosens. Bioelectron.* **2022**, *195* (September 2021), 113649. https://doi.org/10.1016/j.bios.2021.113649.

(22) Yokus, M. A.; Songkakul, T.; Pozdin, V. A.; Bozkurt, A.; Daniele, M. A. Wearable Multiplexed Biosensor System toward Continuous Monitoring of Metabolites. *Biosens. Bioelectron.* **2020**, *153* (January), 112038. https://doi.org/10.1016/j.bios.2020.112038.

(23) Jia, X.; Liu, Z.; Liu, N.; Ma, Z. A Label-Free Immunosensor Based on Graphene Nanocomposites for Simultaneous Multiplexed Electrochemical Determination of Tumor Markers. *Biosens. Bioelectron.* **2014**, *53*, 160–166. https://doi.org/10.1016/j.bios.2013.09.050.

(24) Glatz, R. T.; Ates, H. C.; Mohsenin, H.; Weber, W.; Dincer, C. Designing Electrochemical Microfluidic Multiplexed Biosensors for On-Site Applications. *Anal. Bioanal. Chem.* **2022**, *414* (22), 6531–6540. https://doi.org/10.1007/s00216-022-04210-4.

(25) Le, Z.; Yu, J.; Quek, Y. J.; Bai, B.; Li, X.; Shou, Y.; Myint, B.; Xu, C.; Tay, A. Design Principles of Microneedles for Drug Delivery and Sampling Applications. *Mater. Today* **2023**, *63* (March), 137–169. https://doi.org/10.1016/j.mattod.2022.10.025.

(26) Hu, Y.; Chatzilakou, E.; Pan, Z.; Traverso, G.; Yetisen, A. K. Microneedle Sensors for Point-of-Care Diagnostics. *Adv. Sci.* **2024**, *2306560*, 1–24. https://doi.org/10.1002/advs.202306560.

(27) Liu, G. S.; Kong, Y.; Wang, Y.; Luo, Y.; Fan, X.; Xie, X.; Yang, B. R.; Wu, M. X. Microneedles for Transdermal Diagnostics: Recent Advances and New Horizons. *Biomaterials* **2020**, *232* (December 2019), 119740. https://doi.org/10.1016/j.biomaterials.2019.119740.

(28) Li, H.; Li, H.; Department of Biomedical Engineering, Institute of Materials Science, University of Connecticut, Storrs, Connecticut 06269, U. S.; Li, M. by H.; , Guangfu Wu, Zhengyan Weng, He Sun, Ravi Nistala, and Y. Z. Microneedle-Based Potentiometric Sensing System for Continuous Monitoring of Multiple Electrolytes in Skin Interstitial Fluids. **2021**.

(29) Nagarkar, R.; Singh, M.; Nguyen, H. X.; Jonnalagadda, S. A Review of Recent Advances in Microneedle Technology for Transdermal Drug Delivery. *J. Drug Deliv. Sci. Technol.* **2020**, *59* (July), 101923. https://doi.org/10.1016/j.jddst.2020.101923.

(30) He, X.; Sun, J.; Zhuang, J.; Xu, H.; Liu, Y.; Wu, D. Microneedle System for Transdermal Drug and Vaccine Delivery: Devices, Safety, and Prospects. *Dose-Response* **2019**, *17* (4), 1–18. https://doi.org/10.1177/1559325819878585.

(31) Aldawood, F. K.; Andar, A.; Desai, S. A Comprehensive Review of Microneedles: Types, Materials, Processes, Characterizations and Applications. *Polymers (Basel).* **2021**, *13* (16), 1–34. https://doi.org/10.3390/polym13162815.

(32) Zheng, L.; Zhu, D.; Xiao, Y.; Zheng, X.; Chen, P. Microneedle Coupled Epidermal Sensor for Multiplexed Electrochemical Detection of Kidney Disease Biomarkers. *Biosens. Bioelectron.* **2023**, *237* (June), 115506. https://doi.org/10.1016/j.bios.2023.115506.

(33) Gao, J.; Huang, W.; Chen, Z.; Yi, C.; Jiang, L. Simultaneous Detection of Glucose, Uric Acid and Cholesterol Using Flexible Microneedle Electrode Array-Based Biosensor and Multi-Channel Portable Electrochemical Analyzer. *Sensors Actuators, B Chem.* **2019**, *287* (November 2018), 102–110. https://doi.org/10.1016/j.snb.2019.02.020.

(34) Mugo, S. M.; Robertson, S. V.; Lu, W. A Molecularly Imprinted Electrochemical Microneedle Sensor for Multiplexed Metabolites Detection in Human Sweat. *Talanta* **2023**, *259* (April), 124531. https://doi.org/10.1016/j.talanta.2023.124531.

(35) Muamer Dervisevic, Maria Alba, Li Yan, Mehmet Senel, Thomas R. Gengenbach, Beatriz Prieto-Simon, N. H. V. Transdermal Electrochemical Monitoring of Glucose via High-Density Silicon Microneedle Array Patch. **2021**.

(36) Mishra, R. K.; Goud, K. Y.; Li, Z.; Moonla, C.; Mohamed, M. A.; Tehrani, F.; Teymourian, H.; Wang, J. Continuous Opioid Monitoring along with Nerve Agents on a Wearable Microneedle Sensor Array. *J. Am. Chem. Soc.* **2020**, *142* (13), 5991–5995. https://doi.org/10.1021/jacs.0c01883.

(37) García-Guzmán, J. J.; Pérez-Ràfols, C.; Cuartero, M.; Crespo, G. A. Microneedle Based Electrochemical (Bio)Sensing: Towards Decentralized and Continuous Health Status Monitoring. *TrAC - Trends Anal. Chem.* **2021**, *135*. https://doi.org/10.1016/j.trac.2020.116148.

(38) Jochum, F.; Moltu, S. J.; Senterre, T.; Nomayo, A.; Goulet, O.; Iacobelli, S.; Braegger, C.; Bronsky, J.; Cai, W.; Campoy, C.; Carnielli, V.; Darmaun, D.; Decsi, T.; Domellöf, M.; Embleton, N.; Fewtrell, M.; Fidler Mis, N.; Franz, A.; Goulet, O.; Hartman, C.; Hill, S.; Hojsak, I.; Jochum, F.; Joosten, K.; Kolaček, S.; Koletzko, B.; Ksiazyk, J.; Lapillonne, A.; Lohner, S.; Mesotten, D.; Mihályi, K.; Mihatsch, W. A.; Mimouni, F.; Mølgaard, C.; Moltu, S. J.; Nomayo, A.; Picaud, J. C.; Prell, C.; Puntis, J.; Riskin, A.; Saenz De Pipaon, M.; Shamir, R.; Simchowitz, V.; Szitanyi, P.; Tabbers, M. M.; Van Den Akker, C. H. B.; Van Goudoever, J. B.; Van Kempen, A.; Verbruggen, S.; Wu, J.; Yan, W. ESPGHAN/ESPEN/ESPR/CSPEN Guidelines on Pediatric Parenteral Nutrition: Fluid and Electrolytes. *Clin. Nutr.* **2018**, *37* (6), 2344–2353. https://doi.org/10.1016/j.clnu.2018.06.948.

(39) McNamara, K.; Tofail, S. A. M. Nanoparticles in Biomedical Applications. *Adv. Phys. X* **2017**, *2* (1), 54–88. https://doi.org/10.1080/23746149.2016.1254570.

(40) W. O. Fenn. THE RÔLE OF POTASSIUM IN PHYSIOLOGICAL PROCESSES. **1940**.

(41) Frassetto, L. A.; Goas, A.; Gannon, R.; Lanham-New, S. A.; Lambert, H. Potassium. *Adv. Nutr.* **2023**, *14* (5), 1237–1240. https://doi.org/10.1016/j.advnut.2023.06.004.

(42) Strazzullo, P.; Leclercq, C. Sodium. *Adv. Nutr.* **2014**, *5* (2), 188–190. https://doi.org/10.3945/an.113.005215.

(43) Nguyen, P. T.; Deisl, C.; Fine, M.; Tippetts, T. S.; Uchikawa, E.; Bai, X. chen; Levine, B. Structural Basis for Gating Mechanism of the Human Sodium-Potassium Pump. *Nat. Commun.* **2022**, *13* (1). https://doi.org/10.1038/s41467-022-32990-x.

(44) Aoi, W.; Zou, X.; Xiao, J. B.; Marunaka, Y. Body Fluid PH Balance in Metabolic Health and Possible Benefits of Dietary Alkaline Foods. *eFood* **2020**, *1* (1), 12–23. https://doi.org/10.2991/efood.k.190924.001.

(45) Zhu, J.; Zhou, X.; Libanori, A.; Sun, W. Microneedle-Based Bioassays. *Nanoscale Adv.* **2020**, *2* (10), 4295–4304. https://doi.org/10.1039/d0na00543f.

(46) Aoi, W.; Marunaka, Y. Importance of PH Homeostasis in Metabolic Health and Diseases: Crucial Role of Membrane Proton Transport. *Biomed Res. Int.* **2014**, *2014*, 598986. https://doi.org/10.1155/2014/598986.

(47) Honeychurch, K. C. Printed Thick-Fi Lm Biosensors. **2012**. https://doi.org/10.1533/9780857096210.2.366.

(48) Bontempelli, G.; Dossi, N.; Toniolo, R. Linear Sweep and Cyclic; 2016. https://doi.org/10.1016/B978-0-12-409547-2.12200-0.

(49) Belding, S. R.; Limon-Petersen, J. G.; Dickinson, E. J. F.; Compton, R. G. Cyclic Voltammetry in the Absence of Excess Supporting Electrolyte Offers Extra Kinetic and Mechanistic Insights: Comproportionation of Anthraquinone and the Anthraquinone Dianion in Acetonitrile. *Angew. Chemie - Int. Ed.* **2010**, *49* (48), 9242–9245. https://doi.org/10.1002/anie.201004874.

(50) Chen, A.; Shah, B. Electrochemical Sensing and Biosensing Based on Square Wave Voltammetry. *Anal. Methods* **2013**, *5* (9), 2158–2173. https://doi.org/10.1039/c3ay40155c.

(51) Chen, Z.; Zhou, T.; Zhang, C.; Ma, H.; Lin, Y.; Li, K. Aptasensor for Label-Free Square-Wave Voltammetry Detection of Potassium Ions Based on Gold Nanoparticle Amplification. *RSC Adv.* **2014**, *4* (89), 48671–48675. https://doi.org/10.1039/c4ra05058d.

(52) Charoenkitamorn, K.; Tue, P. T.; Kawai, K.; Chailapakul, O.; Takamura, Y. Electrochemical Immunoassay Using Open Circuit Potential Detection Labeled by Platinum Nanoparticles. *Sensors (Switzerland)* **2018**, *18* (2). https://doi.org/10.3390/s18020444.

(53) Guy, O. J.; Walker, K. A. D. *Graphene Functionalization for Biosensor Applications*, Second Edi.; Elsevier Inc., 2016. https://doi.org/10.1016/B978-0-12-802993-0.00004-6.

(54) Carli, S.; Bianchi, M.; Zucchini, E.; Di Lauro, M.; Prato, M.; Murgia, M.; Fadiga, L.; Biscarini, F. Electrodeposited PEDOT:Nafion Composite for Neural Recording and Stimulation. *Adv. Healthc. Mater.* **2019**, *8* (19), 1–10. https://doi.org/10.1002/adhm.201900765.

(55) Jackson, D. T.; Nelson, P. N. Preparation and Properties of Some Ion Selective Membranes: A Review. *J. Mol. Struct.* **2019**, *1182*, 241–259. https://doi.org/10.1016/j.molstruc.2019.01.050.

(56) Tolosa, V. M.; Wassum, K. M.; Maidment, N. T.; Monbouquette, H. G. Electrochemically Deposited Iridium Oxide Reference Electrode Integrated with an Electroenzymatic Glutamate Sensor on a Multi-Electrode Array Microprobe. *Biosens. Bioelectron.* **2013**, *42* (1), 256–260. https://doi.org/10.1016/j.bios.2012.10.061.

(57) Dhand, C.; Das, M.; Datta, M.; Malhotra, B. D. Recent Advances in Polyaniline Based Biosensors. *Biosens. Bioelectron.* **2011**, *26* (6), 2811–2821. https://doi.org/10.1016/j.bios.2010.10.017.

(58) Yamanaka, K. Anodically Electrodeposited Iridium Oxide Films. *Japanese Journal of Applied Physics*. 1989, pp 632–637.

(59) Shi, J.; Porterfield, D. M. Surface Modification Approaches for Electrochemical Biosensors; Serra, P. A., Ed.; IntechOpen: Rijeka, 2011; p Ch. 11. https://doi.org/10.5772/17770.

(60) Salimi, A.; Hyde, M.; Banks, C.; Compton, R. Boron Doped Diamond Electrode Modified with Iridium Oxide for Amperometic Detection of Ultra Trace Amounts of Arsenic(III). *Analyst* **2004**, *129*, 9–14. https://doi.org/10.1039/B312285A.

(61) Shahrestani, S.; Ismail, M.; Kakooei, S.; Beheshti, M.; Zabihiazadboni, M.; Zavareh, M. Iridium Oxide PH Sensor Based on Stainless Steel Wire for PH Mapping on Metal Surface. *IOP Conf. Ser. Mater. Sci. Eng.* **2018**, *328*, 12014. https://doi.org/10.1088/1757-899X/328/1/012014.

(62) Wu, Z.; Qiao, Z.; Chen, S.; Fan, S.; Liu, Y.; Qi, J.; Lim, C. T. Interstitial Fluid-Based Wearable Biosensors for Minimally Invasive Healthcare and Biomedical Applications. *Commun. Mater.* **2024**, *5* (1). https://doi.org/10.1038/s43246-024-00468-6.

(63) Gojeh - Amrsc Mcsn Masfi Mpin, M.; Bahago, N.; Yilleng, M.; Adisu, S.; Jabason, S. Electrochemical Modification Of Carbon Paste Electrode Using Polyaniline And Gold Particles For Signal Enhancement. **2015**, *8*, 1–6. https://doi.org/10.9790/5736-08910106.

(64) García-Guzmán, J. J.; Pérez-Ràfols, C.; Cuartero, M.; Crespo, G. A. Toward in Vivo Transdermal PH Sensing with a Validated Microneedle Membrane Electrode. *ACS Sensors* **2021**, *6* (3), 1129–1137. https://doi.org/10.1021/acssensors.0c02397.